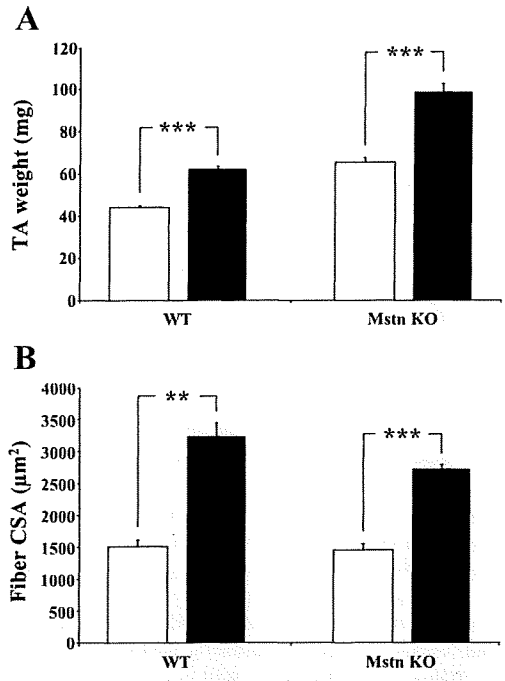

Fig. 3. Overexpression of FS induces comparable muscle (*A*) and fiber (*B*) hypertrophy in wild-type (WT) and myostatin-knockout (Mstn-KO) mice. TA mass and fiber CSA were measured 17 days after transfection of pM1 (open bars) or pM1-FS288 (filled bars). The results are expressed as means ± SE. $^{**}P < 0.01$ and $^{***}P < 0.001$.

DISCUSSION

Our study shows that FS overexpression induces skeletal muscle hypertrophy via satellite cell activation and probably increased protein synthesis. Furthermore, our results indicate that FS-induced hypertrophy results not only from Mstn but also from Act inhibition. Therefore, these observations suggest that, besides Mstn, Act is a crucial player in the regulation of muscle mass.

FS-induced hypertrophy was characterized by increased fiber diameter together with DNA and protein accretion. Muscle DNA content reflects the number of myonuclei, including satellite cell nuclei. Therefore, increased DNA content, as we observed, reflects an increase in the number of myonuclei, which is dependent on satellite cell replication. This is entirely consistent with the observation of increased PCNA expression after FS overexpression. In addition, the differentiation of the satellite cells into new muscle fibers was attested by increased neonatal MHC expression, a marker of myogenesis. On the other hand, increased muscle protein content probably reflects accelerated protein synthesis, in particular of myofibrillar proteins such as MHCIIb, as suggested by increased MHCIIb mRNA. Indeed, infusion of FS has been reported to increase muscle protein synthesis in neonatal rats (41). All of these changes that we observed strongly suggest that FS induces muscle hypertrophy by inhibiting Mstn. Indeed, Mstn has been reported to inhibit satellite cell proliferation (38, 43) and differentiation (16) as well as protein synthesis (42, 47, 48), in particular MHCIIb (12). Furthermore, Mstn is abundantly expressed in TA muscle, a muscle composed mainly of IIb myofibers that strongly express Mstn (5, 32). These results are in accordance with previous studies that showed that FS overexpression, either by transgenesis or AAV-mediated gene delivery, causes a dramatic increase in muscle mass (11, 19). However, in these studies only the long-term effect of FS overexpression was considered, in contrast to our study reporting a marked muscle hypertrophy occurring as early as after 17 days.

The implication of satellite cells in the FS-induced muscle hypertrophy, suggested by the increased DNA and PCNA mRNA contents, was directly assessed by the destruction of their proliferative capacity using γ-irradiation. By combining γ-irradiation with FS gene transfer, we were able to tease apart the mechanisms by which muscle hypertrophy is induced by FS. Our results indicate that satellite cells contribute to the FS-induced hypertrophy but that FS is still able to stimulate muscle growth even when their proliferative capacity has been destroyed. This observation suggests that FS causes muscle hypertrophy by stimulating muscle protein synthesis, a hypothesis that was demonstrated recently (41). We are confident that irradiation achieved blockade of satellite cell activation, since DNA synthesis assessed by Brdu staining was dramatically reduced in irradiated muscle. Since the action of Mstn on muscle development relies heavily on its ability to downregulate satellite cell activity (22, 38), our interpretation is that FS causes muscle hypertrophy by inhibiting Mstn. Interestingly, muscle hypertrophy induced by IGF-I, an anabolic growth factor, is also mediated by a combination of satellite cell proliferation and increased protein synthesis (2). Therefore, this work is the first to demonstrate the contribution of satellite cells in FS-induced muscle hypertrophy.

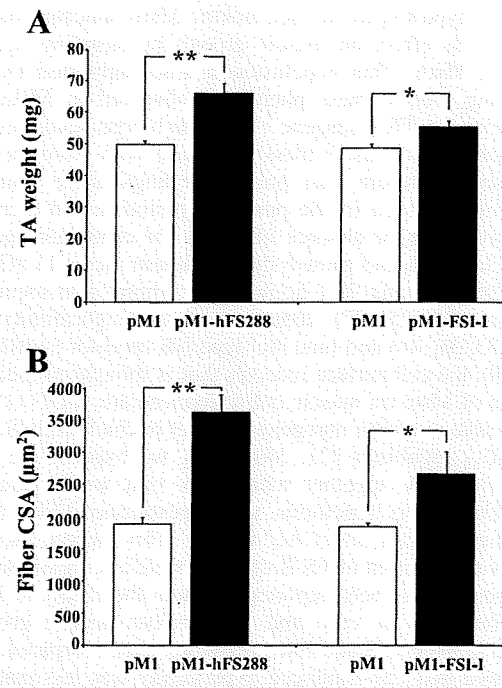

Fig. 4. Overexpression of FSI-I induces a smaller muscle (*A*) and fiber (*B*) hypertrophy than FS288 in WT mice. TA mass and fiber CSA were measured 17 days after transfection of pM1 (open bars) or pM1-hFS288/pM1-FSI-I (filled bars). The results are expressed as means ± SE. $^{*}P < 0.05$ and $^{**}P < 0.01$.

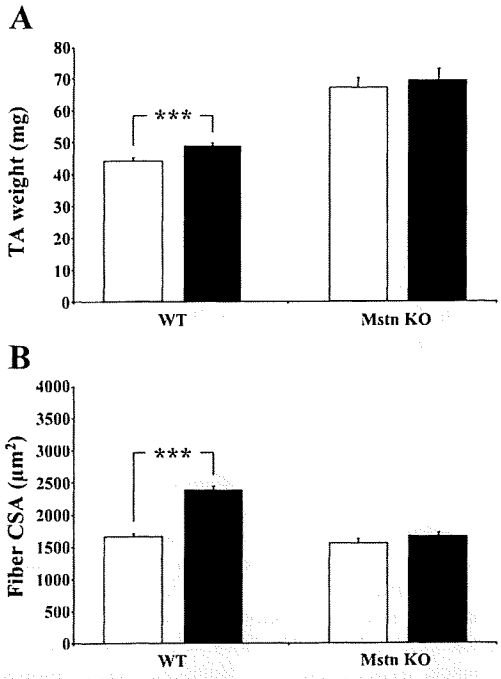

Fig. 5. Overexpression of FSI-I fails to cause muscle (*A*) and fiber (*B*) hypertrophy in Mstn-KO mice. No increase in muscle mass or in fiber CSA was observed in muscle overexpressing FSI-I in Mstn-KO mice compared with WT mice. TA mass and fiber CSA were measured 17 days after the transfection of pM1 (open bars) or pM1-FSI-I (filled bars). The results are expressed as means ± SE. ***$P < 0.001$.

The observation that FS overexpression can cause substantial muscle hypertrophy in mice lacking Mstn indicates that FS must exert its effect on muscle growth by targeting ligands other than Mstn. This conclusion is also supported by the quadrupling muscle mass phenotype observed in Mstn-KO mice carrying a FS transgene (18), which represents yet another doubling of muscle mass compared with mice lacking only Mstn. Therefore, our present findings argue that FS overexpression, even in the postnatal period, could increase muscle growth in the absence of Mstn. The candidate ligands could include Act and growth differentiation factor 11 (GDF-11), the latter sharing 90% homology in amino acid sequence with Mstn (24, 25, 27). Indeed, both are high-affinity FS ligands (35, 36, 44) and bind Act type IIB receptor (ActIIRB) (6, 29, 39), the cell surface receptor that is thought to mediate the action of Mstn on muscle cells. Furthermore, GDF-11 and ActA are able to inhibit myogenesis either in chick limb (9, 13) or in C_2C_{12} myoblasts (21, 39). Thus, we hypothesize that GDF-11 or ActA, together with Mstn, may inhibit muscle growth. To test this hypothesis, we overexpressed FSI-I, a FS mutant that does not affect Act activity. This mutant, characterized by the deletion of FS-II domain, which is important for binding to Act, has been reported to retain the ability to bind and inhibit Mstn in vitro and to stimulate muscle growth in vivo (28). When FS and FSI-I activities were compared, our data showed that FSI-I-induced hypertrophy was less marked than that induced by native FS, consistent with the smaller increase in muscle mass observed in FSI-I transgenic mice (28) compared with FS transgenic mice (18). This difference in the extent of hypertrophy points to a key role of Act inhibition in the FS effect. On the other hand, since FSI-I, which does not bind Act with high affinity, is still able to cause hypertrophy, our data also support the role of Mstn or GDF-11 inhibition in the FSI-I-induced hypertrophy. Indeed, mutants for Mstn over Act, such as FSI-I, are similarly selective for Mstn and GDF-11. However, the fact that FSI-I overexpression in Mstn-KO mice lost its ability to stimulate muscle growth suggests that GDF-11 does not play a major role. In accordance with our results, recent data show that deletion of GDF-11 specifically in skeletal muscle does not affect muscle size, fiber number, or fiber type (23). Taken together, our observations suggest that inhibition of Act may contribute to the muscle hypertrophy caused by FS.

To directly assess the action of Act on postnatal skeletal muscle, we investigated the effect of ActA overexpression on muscle mass. Our results are the first to demonstrate that increased muscle ActA expression causes muscle atrophy. Although the mechanisms involved are not yet described, it is likely that this atrophy resulted from activation of the ActIIRB and ActIIRA, as described for Mstn. Recent data reported that Mstn causes muscle atrophy by downregulating the Akt/mTOR pathway, leading to blunted protein synthesis (1). Because ActA is expressed in skeletal muscle, the possibility therefore exists that ActA controls muscle growth in an autocrine/paracrine manner. Further work will certainly be necessary to delineate the respective roles of Mstn and ActA in the regulation of muscle mass and development. Nevertheless, the study presented here demonstrates that the capacity of promoting muscle growth by targeting this pathway goes beyond the targeting of Mstn alone.

In our work, we demonstrated the hypertrophic effect of FS288. However, two isoforms of FS, FS288 and FS315, are

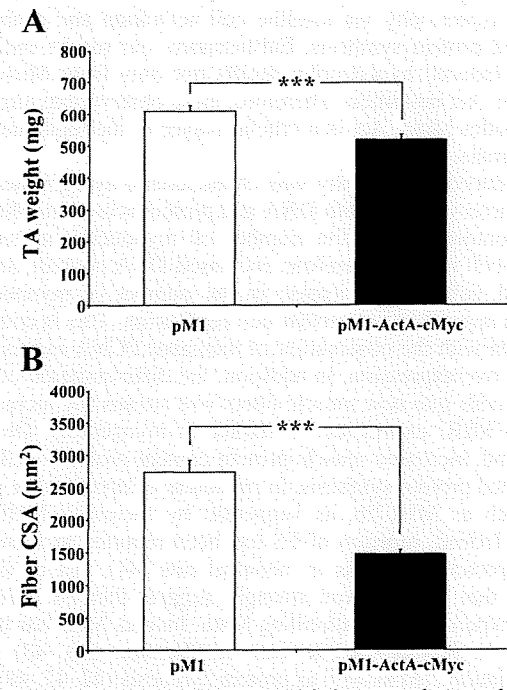

Fig. 6. Overexpression of activin A (ActA) induces muscle (*A*) and fiber (*B*) atrophy in rat. TA mass and fiber CSA were measured 17 days after transfection of pM1 (open bars) or pM1-ActA-c-Myc (filled bars). The results are expressed as means ± SE. ***$P < 0.001$.

generated by alternative splicing. The structural difference between the two forms is the absence of a carboxy-terminal 27-amino acid sequence in the FS288. The FS288 isoform, lacking the COOH terminus, shows high tissue-binding affinity through heparin sulfate proteoglycans via a highly basic region located in FS-I domain (14, 15). However, this basic region is structurally hidden in the FS315 by the COOH-terminal region, precluding the binding of this FS long isoform to extracellular matrix. Because the short form is trapped by the extracellular matrix of the cell transfected (or the neighboring transfected cells), it is therefore less diluted in the circulation. Thus, for our experiments, the FS288 isoform seemed more suitable to inhibit local Mstn. Although FS288 has been reported to block Act activity more effectively than FS315 (40), the two isoforms seem equally effective in inhibiting Mstn bioactivity in vitro (36). Up until now, the hypertrophic action of these two FS isoforms has not yet been compared side by side. Nevertheless, when delivered by intramuscular injection of AAV, FS315 increased the muscle mass and led to functional improvement in dystrophic mice (11). Thus, combining our findings together with the existing data in the literature, we may conclude that muscle overexpression of both FS isoforms enhances muscle mass.

Several observations support the physiological role of FS in the control of muscle mass. Indeed, recent observations suggest that FS may play an essential role in mediating the myogenic effect of androgens (37), a family of very potent anabolic agents. Furthermore, although the role of FS in determining skeletal mass in humans has not yet been explored directly, recent evidence shows associations between haplotype structures of the FS gene with skeletal muscle mass and strength phenotypes (46). Furthermore, FS may be a target for the pharmacological treatment of muscle atrophy. Indeed, the beneficial effect of the administration of histone deacetylase inhibitors (26) or nitric oxide (30) in counteracting the progression of muscular dystrophy in the *mdx* model relies in part on the transcriptional activation of FS. Therefore, in addition to FS itself, FS inducers may represent a new avenue for the treatment of these debilitating conditions. Altogether, these studies pinpoint the role of FS as a physiological regulator of muscle mass and as a molecular target for future drug development.

In conclusion, we showed that satellite cell proliferation significantly contributes to the FS-induced muscle growth. In addition, we showed that the hypertrophic effect results from inhibition of both Mstn and Act, implicating Act as a novel potent regulator of muscle growth. Therefore, the striking ability of FS to enhance muscle growth warrants its consideration as a physiological regulator of muscle mass and as a molecular target for future drug development.

ACKNOWLEDGMENTS

We thank Dr. L. Grobet (Unité d'Embryologie, Faculté de Médecine Vétérinaire, Université de Liège) for the Mstn-KO mice, and we are grateful to Noémie Decroly for assistance in animal care and manipulation. We gratefully acknowledge the collaboration of Prof. J. Lebacq (Laboratoire de Physiologie Cellulaire, Université Catholique de Louvain), Prof. M. C. Many (Unité de Morphologie Expérimentale, Université Catholique de Louvain), Prof. Veronique Préat (Unité de Pharmacie Galénique, Industrielle et Officinale, Université Catholique de Louvain), Prof. V. Grégoire (Unité d'Imagerie Moléculaire et Radiothérapie Expérimentale, Université Catholique de Louvain), and the Pathology Department of Saint-Luc Academic Hospital (Brussels, Belgium), especially Prof. Yves Guiot, for helpful discussion and technical assistance.

GRANTS

H. Gilson is the recipient of a research fellowship from Fonds pour la formation à la Recherche dans l'Industrie et l'Agriculture from the Communauté Française (Belgium). This work was supported by grants from the Fonds de la Recherche Scientifique Médicale (Belgium), the National Fund for Scientific Research (Belgium), the Association Française contre les Myopathies (France), the Association Belge contre les Maladies neuro-Musculaires (Belgium) and the Fonds Spéciaux de Recherche (Université Catholique de Louvain, Belgium).

REFERENCES

1. **Amirouche A, Durieux AC, Banzet S, Koulmann N, Bonnefoy R, Mouret C, Bigard X, Peinnequin A, Freyssenet D.** Down-regulation of Akt/mammalian target of rapamycin signaling pathway in response to myostatin overexpression in skeletal muscle. *Endocrinology* 150: 286–294, 2009.
2. **Barton-Davis ER, Shoturma DI, Sweeney HL.** Contribution of satellite cells to IGF-I induced hypertrophy of skeletal muscle. *Acta Physiol Scand* 167: 301–305, 1999.
3. **Bloquel C, Fabre E, Bureau MF, Scherman D.** Plasmid DNA electrotransfer for intracellular and secreted proteins expression: new methodological developments and applications. *J Gene Med* 6, *Suppl* 1: S11–S23, 2004.
4. **Bogdanovich S, Krag TO, Barton ER, Morris LD, Whittemore LA, Ahima RS, Khurana TS.** Functional improvement of dystrophic muscle by myostatin blockade. *Nature* 420: 418–421, 2002.
5. **Carlson CJ, Booth FW, Gordon SE.** Skeletal muscle myostatin mRNA expression is fiber-type specific and increases during hindlimb unloading. *Am J Physiol Regul Integr Comp Physiol* 277: R601–R606, 1999.
6. **de Caestecker M.** The transforming growth factor-beta superfamily of receptors. *Cytokine Growth Factor Rev* 15: 1–11, 2004.
7. **Dehoux MJ, van Beneden RP, Fernández-Celemín L, Lause PL, Thissen JP.** Induction of MafBx and Murf ubiquitin ligase mRNAs in rat skeletal muscle after LPS injection. *FEBS Lett* 544: 214–217, 2003.
8. **Durieux AC, Amirouche A, Banzet S, Koulmann N, Bonnefoy R, Pasdeloup M, Mouret C, Bigard X, Peinnequin A, Freyssenet D.** Ectopic expression of myostatin induces atrophy of adult skeletal muscle by decreasing muscle gene expression. *Endocrinology* 148: 3140–3147, 2007.
9. **Gamer LW, Cox KA, Small C, Rosen V.** Gdf11 is a negative regulator of chondrogenesis and myogenesis in the developing chick limb. *Dev Biol* 229: 407–420, 2001.
10. **Grobet L, Pirottin D, Farnir F, Poncelet D, Royo LJ, Brouwers B, Christians E, Desmecht D, Coignoul F, Kahn R, Georges M.** Modulating skeletal muscle mass by postnatal, muscle-specific inactivation of the myostatin gene. *Genesis* 35: 227–238, 2003.
11. **Haidet AM, Rizo L, Handy C, Umapathi P, Eagle A, Shilling C, Boue D, Martin PT, Sahenk Z, Mendell JR, Kaspar BK.** Long-term enhancement of skeletal muscle mass and strength by single gene administration of myostatin inhibitors. *Proc Natl Acad Sci USA* 105: 4318–4322, 2008.
12. **Hayashi S, Miyake M, Watanabe K, Aso H, Hayashi S, Ohwada S, Yamaguchi T.** Myostatin preferentially down-regulates the expression of fast 2x myosin heavy chain in cattle. *Proc Jpn Acad Ser B Phys Biol Sci* 84: 354–362, 2008.
13. **He L, Vichev K, Macharia R, Huang R, Christ B, Patel K, Amthor H.** Activin A inhibits formation of skeletal muscle during chick development. *Anat Embryol (Berl)* 209: 401–407, 2005.
14. **Innis CA, Hyvonen M.** Crystal structures of the heparan sulfate-binding domain of follistatin. Insights into ligand binding. *J Biol Chem* 278: 39969–39977, 2003.
15. **Inouye S, Ling N, Shimasaki S.** Localization of the heparin binding site of follistatin. *Mol Cell Endocrinol* 90: 1–6, 1992.
16. **Langley B, Thomas M, Bishop A, Sharma M, Gilmour S, Kambadur R.** Myostatin inhibits myoblast differentiation by down regulating MyoD expression. *J Biol Chem* 277: 49831–49840, 2002.
18. **Lee SJ.** Quadrupling muscle mass in mice by targeting TGF-beta signaling pathways. *PLoS ONE* 2: e789, 2007.
19. **Lee SJ, McPherron AC.** Regulation of myostatin activity and muscle growth. *Proc Natl Acad Sci USA* 98: 9306–9311, 2001.
20. **Lewis RB.** Changes in striated muscle following single intense doses of x-rays. *Lab Invest* 3: 48–55, 1954.
21. **Link BA, Nishi R.** Opposing effects of activin A and follistatin on developing skeletal muscle cells. *Exp Cell Res* 233: 350–362, 1997.

22. **McCroskery S, Thomas M, Maxwell L, Sharma M, Kambadur R.** Myostatin negatively regulates satellite cell activation and self-renewal. *J Cell Biol* 162: 1135–1147, 2003.
23. **McPherron AC, Huynh TV, Lee SJ.** Redundancy of myostatin and growth/differentiation factor 11 function. *BMC Dev Biol* 9: 24, 2009.
24. **McPherron AC, Lawler AM, Lee SJ.** Regulation of skeletal muscle mass in mice by a new TGF-beta superfamily member. *Nature* 387: 83–90, 1997.
25. **McPherron AC, Lawler AM, Lee SJ.** Regulation of anterior/posterior patterning of the axial skeleton by growth/differentiation factor 11. *Nat Genet* 22: 260–264, 1999.
26. **Minetti GC, Colussi C, Adami R, Serra C, Mozzetta C, Parente V, Fortuni S, Straino S, Sampaolesi M, Di Padova M, Illi B, Gallinari P, Steinkuhler C, Capogrossi MC, Sartorelli V, Bottinelli R, Gaetano C, Puri PL.** Functional and morphological recovery of dystrophic muscles in mice treated with deacetylase inhibitors. *Nat Med* 12: 1147–1150, 2006.
27. **Nakashima M, Toyono T, Akamine A, Joyner A.** Expression of growth/differentiation factor 11, a new member of the BMP/TGFbeta superfamily during mouse embryogenesis. *Mech Dev* 80: 185–189, 1999.
28. **Nakatani M, Takehara Y, Sugino H, Matsumoto M, Hashimoto O, Hasegawa Y, Murakami T, Uezumi A, Takeda S, Noji S, Sunada Y, Tsuchida K.** Transgenic expression of a myostatin inhibitor derived from follistatin increases skeletal muscle mass and ameliorates dystrophic pathology in mdx mice. *FASEB J* 22: 477–487, 2008.
29. **Oh SP, Yeo CY, Lee Y, Schrewe H, Whitman M, Li E.** Activin type IIA and IIB receptors mediate Gdf11 signaling in axial vertebral patterning. *Genes Dev* 16: 2749–2754, 2002.
30. **Pisconti A, Brunelli S, Di Padova M, De Palma C, Deponti D, Baesso S, Sartorelli V, Cossu G, Clementi E.** Follistatin induction by nitric oxide through cyclic GMP: a tightly regulated signaling pathway that controls myoblast fusion. *J Cell Biol* 172: 233–244, 2006.
31. **Reisz-Porszasz S, Bhasin S, Artaza JN, Shen R, Sinha-Hikim I, Hogue A, Fielder TJ, Gonzalez-Cadavid NF.** Lower skeletal muscle mass in male transgenic mice with muscle-specific overexpression of myostatin. *Am J Physiol Endocrinol Metab* 285: E876–E888, 2003.
32. **Salerno MS, Thomas M, Forbes D, Watson T, Kambadur R, Sharma M.** Molecular analysis of fiber type-specific expression of murine myostatin promoter. *Am J Physiol Cell Physiol* 287: C1031–C1040, 2004.
33. **Schakman O, Gilson H, de Coninck V, Lause P, Verniers J, Havaux X, Ketelslegers JM, Thissen JP.** Insulin-like growth factor-I gene transfer by electroporation prevents skeletal muscle atrophy in glucocorticoid-treated rats. *Endocrinology* 146: 1789–1797, 2005.
34. **Schakman O, Kalista S, Bertrand L, Lause P, Verniers J, Ketelslegers JM, Thissen JP.** Role of Akt/GSK-3beta/beta-catenin transduction pathway in the muscle anti-atrophy action of insulin-like growth factor-I in glucocorticoid-treated rats. *Endocrinology* 149: 3900–3908, 2008.
35. **Schneyer AL, Rzucidlo DA, Sluss PM, Crowley WF Jr.** Characterization of unique binding kinetics of follistatin and activin or inhibin in serum. *Endocrinology* 135: 667–674, 1994.
36. **Sidis Y, Mukherjee A, Keutmann H, Delbaere A, Sadatsuki M, Schneyer A.** Biological activity of follistatin isoforms and follistatin-like-3 is dependent on differential cell surface binding and specificity for activin, myostatin, and bone morphogenetic proteins. *Endocrinology* 147: 3586–3597, 2006.
37. **Singh R, Bhasin S, Braga M, Artaza JN, Pervin S, Taylor WE, Krishnan V, Sinha SK, Rajavashisth TB, Jasuja R.** Regulation of myogenic differentiation by androgens: cross talk between androgen receptor/ beta-catenin and follistatin/transforming growth factor-beta signaling pathways. *Endocrinology* 150: 1259–1268, 2009.
38. **Siriett V, Platt L, Salerno MS, Ling N, Kambadur R, Sharma M.** Prolonged absence of myostatin reduces sarcopenia. *J Cell Physiol* 209: 866–873, 2006.
39. **Souza TA, Chen X, Guo Y, Sava P, Zhang J, Hill JJ, Yaworsky PJ, Qiu Y.** Proteomic identification and functional validation of activins and bone morphogenetic protein 11 as candidate novel muscle mass regulators. *Mol Endocrinol* 22: 2689–2702, 2008.
40. **Sugino H, Sugino K, Hashimoto O, Shoji H, Nakamura T.** Follistatin and its role as an activin-binding protein. *J Med Invest* 44: 1–14, 1997.
41. **Suryawan A, Frank JW, Nguyen HV, Davis TA.** Expression of the TGF-beta family of ligands is developmentally regulated in skeletal muscle of neonatal rats. *Pediatr Res* 59: 175–179, 2006.
42. **Taylor WE, Bhasin S, Artaza J, Byhower F, Azam M, Willard DH Jr, Kull FC Jr, Gonzalez-Cadavid N.** Myostatin inhibits cell proliferation and protein synthesis in C_2C_{12} muscle cells. *Am J Physiol Endocrinol Metab* 280: E221–E228, 2001.
43. **Thomas M, Langley B, Berry C, Sharma M, Kirk S, Bass J, Kambadur R.** Myostatin, a negative regulator of muscle growth, functions by inhibiting myoblast proliferation. *J Biol Chem* 275: 40235–40243, 2000.
44. **Tortoriello DV, Sidis Y, Holtzman DA, Holmes WE, Schneyer AL.** Human follistatin-related protein: a structural homologue of follistatin with nuclear localization. *Endocrinology* 142: 3426–3434, 2001.
45. **Wagner KR, McPherron AC, Winik N, Lee SJ.** Loss of myostatin attenuates severity of muscular dystrophy in mdx mice. *Ann Neurol* 52: 832–836, 2002.
46. **Walsh S, Metter EJ, Ferrucci L, Roth SM.** Activin-type II receptor B (*ACVR2B*) and *follistatin* haplotype associations with muscle mass and strength in humans. *J Appl Physiol* 102: 2142–2148, 2007.
47. **Welle S, Bhatt K, Pinkert CA.** Myofibrillar protein synthesis in myostatin-deficient mice. *Am J Physiol Endocrinol Metab* 290: E409–E415, 2006.
48. **Welle S, Burgess K, Mehta S.** Stimulation of skeletal muscle myofibrillar protein synthesis, p70 S6 kinase phosphorylation, and ribosomal protein S6 phosphorylation by inhibition of myostatin in mature mice. *Am J Physiol Endocrinol Metab* 296: E567–E572, 2009.

Activin A and Follistatin-Like 3 Determine the Susceptibility of Heart to Ischemic Injury

Yuichi Oshima, MD, PhD; Noriyuki Ouchi, MD, PhD; Masayuki Shimano, MD, PhD; David R. Pimentel, MD; Kyriakos N. Papanicolaou, BSc; Kalyani D. Panse, MSc; Kunihiro Tsuchida, MD, PhD; Enrique Lara-Pezzi, PhD; Se-Jin Lee, MD, PhD; Kenneth Walsh, PhD

Background—Transforming growth factor-β family cytokines have diverse actions in the maintenance of cardiac homeostasis. Activin A is a member of this family whose regulation and function in heart are not well understood at a molecular level. Follistatin-like 3 (Fstl3) is an extracellular regulator of activin A protein, and its function in the heart is also unknown.

Methods and Results—We analyzed the expression of various transforming growth factor-β superfamily cytokines and their binding partners in mouse heart. *Activin βA* and *Fstl3* were upregulated in models of myocardial injury. Overexpression of activin A with an adenoviral vector (Ad-actβA) or treatment with recombinant activin A protein protected cultured myocytes from hypoxia/reoxygenation-induced apoptosis. Systemic overexpression of activin A in mice by intravenous injection of Ad-actβA protected hearts from ischemia/reperfusion injury. Activin A induced the expression of Bcl-2, and ablation of Bcl-2 by small interfering RNA abrogated its protective action in myocytes. The protective effect of activin A on cultured myocytes was abolished by treatment with Fstl3 or by a pharmacological activin receptor-like kinase inhibitor. Cardiac-specific *Fstl3* knockout mice showed significantly smaller infarcts after ischemia/reperfusion injury that was accompanied by reduced apoptosis.

Conclusions—Activin A and Fstl3 are induced in heart by myocardial stress. Activin A protects myocytes from death, and this activity is antagonized by Fstl3. Thus, the relative expression levels of these factors after injury is a determinant of cell survival in the heart. (***Circulation.*** **2009;120:1606-1615.)**

Key Words: activin A ■ apoptosis ■ follistatin-like 3 ■ myocytes ■ reperfusion

The transforming growth factor-β (TGF-β) family comprises a large number of multifunctional proteins that can be divided into subfamilies including activins, bone morphogenic proteins, growth and differentiation factors (GDFs), and TGF-βs. These secreted proteins have diverse roles in cell proliferation, differentiation, apoptosis, and immune responses.[1] TGF-β1, the founding member of the TGF-β superfamily, is a mediator of cardiac hypertrophy and remodeling.[2,3] It has also been reported that bone morphogenic protein-2,[4,5] GDF-15,[6,7] and myostatin (GDF-8)[8] influence the growth and survival of cardiac myocytes. However, the majority of TGF-β superfamily members have not been examined for their potential cardiac-regulatory functions.

Clinical Perspective on p 1615

The follistatin family proteins function as extracellular antagonists of TGF-β superfamily cytokines. Follistatin and follistatin-like 3 (Fstl3) bind directly to TGF-β superfamily cytokines to inhibit their biological activities.[1] Recently, Lara-Pezzi et al[9] reported that *Fstl3* transcript expression is upregulated in end-stage failing myocardium and its expression is correlated with molecular markers of disease severity. They also reported that transcripts encoding follistatin-like 1 (Fstl1), a distant member of the follistatin family, are upregulated in heart failure and expression is positively correlated with better functional recovery after implantation of a left ventricular assist device. We have shown that Fstl1 is secreted from cardiac myocytes after injury in animal models and that it functions to promote cardiac myocyte survival.[10]

To better understand the regulation of secreted factors from the heart, we performed gene array transcriptome analyses on murine hearts that were subjected to injury and other stimuli.[11,12] These analyses revealed that members of the follistatin family of secreted factors were upregulated on injury or Akt

Received April 9, 2009; accepted August 13, 2009.

From the Molecular Cardiology Unit, Whitaker Cardiovascular Institute (Y.O., N.O., M.S., K.N.P., K.W.), and the Myocardial Biology Unit (D.R.P.), Boston University Medical Campus, Boston, Mass; Imperial College London, Heart Science Centre, Harefield, United Kingdom (K.D.P., E.L.-P.); Division for Therapies Against Intractable Diseases, Institute for Comprehensive Medical Sciences, Fujita Health University, Toyoake, Japan (K.T.); and Department of Molecular Biology and Genetics, Johns Hopkins University School of Medicine, Baltimore, Md (S.L.).

Guest Editor for this article was Douglas L. Mann, MD.

The online-only Data Supplement is available with this article at http://circ.ahajournals.org/cgi/content/full/CIRCULATIONAHA.109.872200/DC1.

Correspondence to Kenneth Walsh, PhD, Molecular Cardiology Unit/Whitaker Cardiovascular Institute, Boston University Medical Campus, 700 Albany St, W611, Boston, MA 02118. E-mail kxwalsh@bu.edu

Circulation **is available at http://circ.ahajournals.org** **DOI: 10.1161/CIRCULATIONAHA.109.872200**

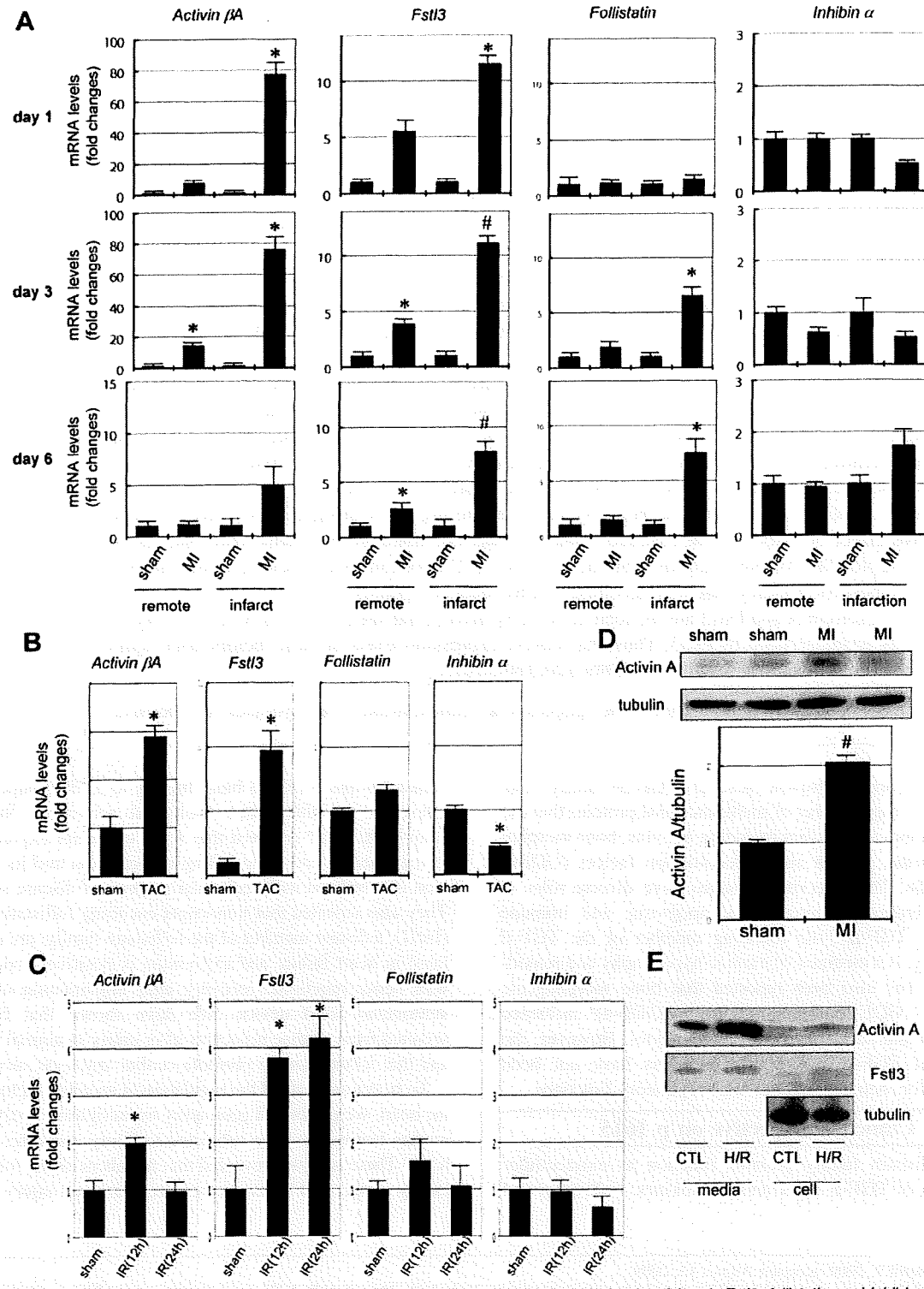

Figure 1. *Fstl3* and *Activin βA* are specifically induced after cardiac injury. Expression analysis of *activin βA*, *Fstl3*, *follistatin*, and *inhibin α* in murine models of myocardial infarction (MI) (A), transverse aortic constriction (TAC) (B), and I/R (IR) (C) is shown. In the myocardial infarction model, samples were taken separately from ischemic zone (infarct area) and nonischemic zone (remote area) 3 days after the onset of myocardial infarction. For the pressure overload model, samples were taken 7 days after transverse aortic constriction surgery. Quantitative real-time polymerase chain reaction was performed to determine the mRNA level of each transcript, and the data were compared with the GAPDH level and normalized to the mean value of controls. n=4 to 6. *$P<0.05$ vs sham; #$P<0.01$ vs sham. D, Upregulation of activin A protein after myocardial infarction. The top panel is a Western blot analysis for activin A performed under nonreducing conditions, and the bottom panel is a blot for α-tubulin with the same samples used under reducing conditions. The histogram shows the quantification of the band intensities for activin A compared with that of tubulin. #$P<0.01$ vs sham. E, Upregulation of activin A and Fstl3 proteins after H/R treatment in NRVM cultures. Representative images of immunoblots of the culture media, 24 hours after addition to cells, and the cell pellet lysates are shown. CTL indicates control.

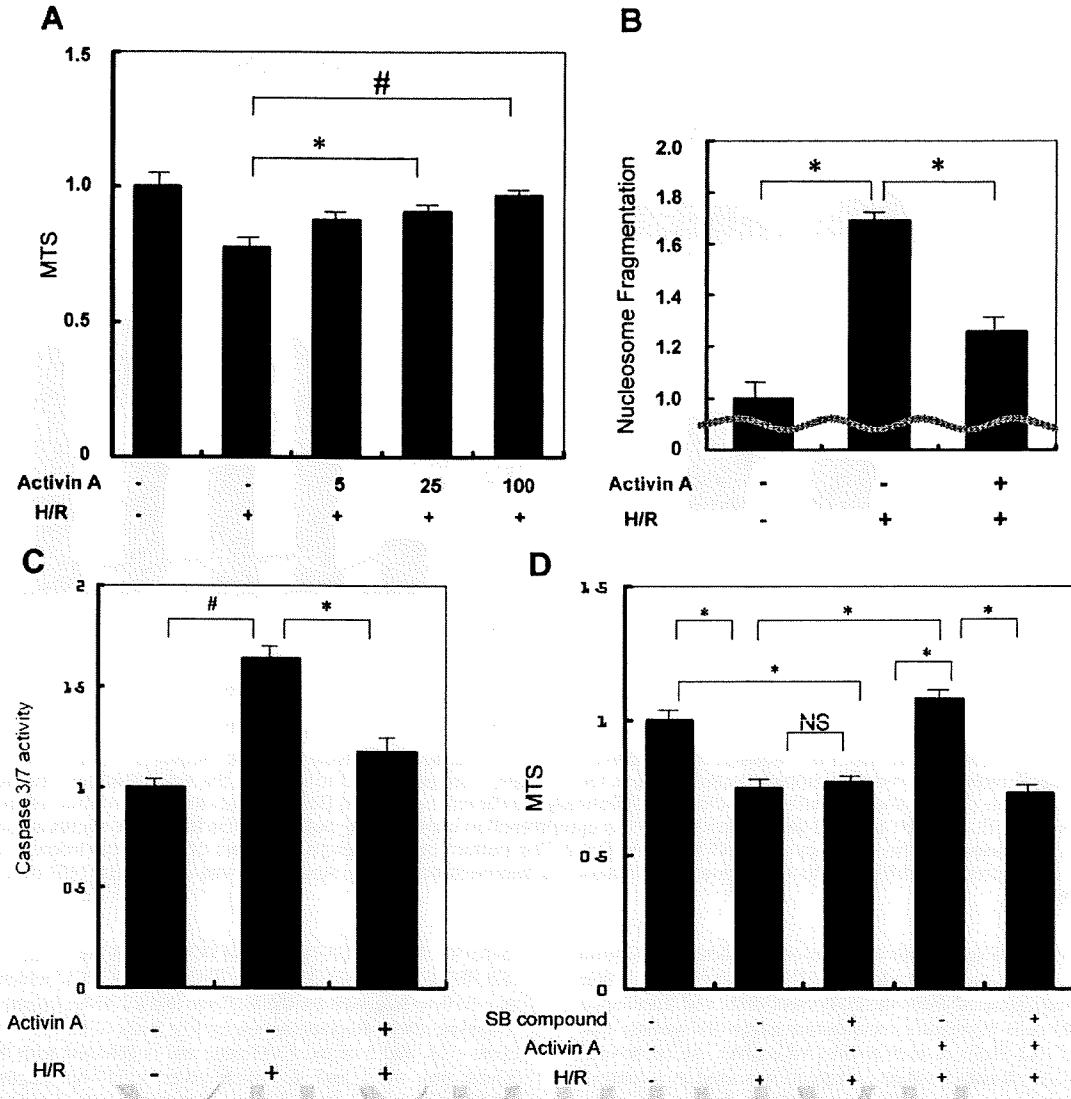

Figure 2. Activin A protects cardiac myocytes from H/R-induced injury. A, NRVMs were pretreated with different concentrations of activin A for 8 hours before the exposure to 12 hours of hypoxia followed by 24 hours of reoxygenation (H/R). Cell viability was determined by the MTS assay. Apoptosis indicated by nucleosome fragmentation assay (B) and caspase-3 and -7 activities (C) were measured in NRVMs pretreated with 25 ng/mL of activin A before exposure to H/R. D, Thirty minutes before addition of activin A, NRVMs were pretreated with or without the inhibitor SB431542 (SB). Cell viability was measured by MTS assay after H/R treatment. *$P<0.05$; #$P<0.01$.

transgene activation,[10] leading us to hypothesize that there might exist as yet unknown networks of autocrine/paracrine factors that control heart function. In this study, we report that cardiac injuries induce the expression of activin A and its binding partner Fstl3. Activin A was found to protect cardiac myocytes from stress-induced cell death, whereas Fstl3 abolished the prosurvival effect of activin A. We propose that activin A and Fstl3 serve as sensors of cardiac stress and that their relative levels of expression influence cell survival in the injured heart.

Methods

See the online-only Data Supplement for additional details.

Myocyte Cultures of Neonatal Rat Ventricular Myocytes

Primary cultures of neonatal rat ventricular myocytes (NRVMs) were incubated in Dulbecco's modified Eagle's medium supplemented with 7% fetal calf serum for 18 to 24 hours after preparation, then with adenoviral vectors at the indicated multiplicity of infection (MOI) for 16 hours in Dulbecco's modified Eagle's medium. The media were then replaced with fresh DMEM without adenovirus and incubated for 12 hours before hypoxia/reoxygenation (H/R). In other experiments, serum-deprived NRVMs were incubated with recombinant activin A protein for 8 hours before H/R. A GasPak system (Becton Dickinson) was used to create hypoxic conditions as described previously.[13] For H/R studies, cells were exposed to 12 hours of hypoxia followed by reoxygenation.

Construction of Adenoviral Vectors Expressing Murine Fstl3 and Murine Activin βA

Full-length *Fstl3* and *activin βA* complementary DNAs (cDNAs) were obtained from American Type Culture Collection. Enzymatic restriction sites were added by polymerase chain reaction on both N- and C-terminus, and the full length of *Fstl3* and *activin βA* and the cDNAs were subcloned into an adenovirus shuttle vector. After linearization, the shuttle vectors were cotransformed into competent

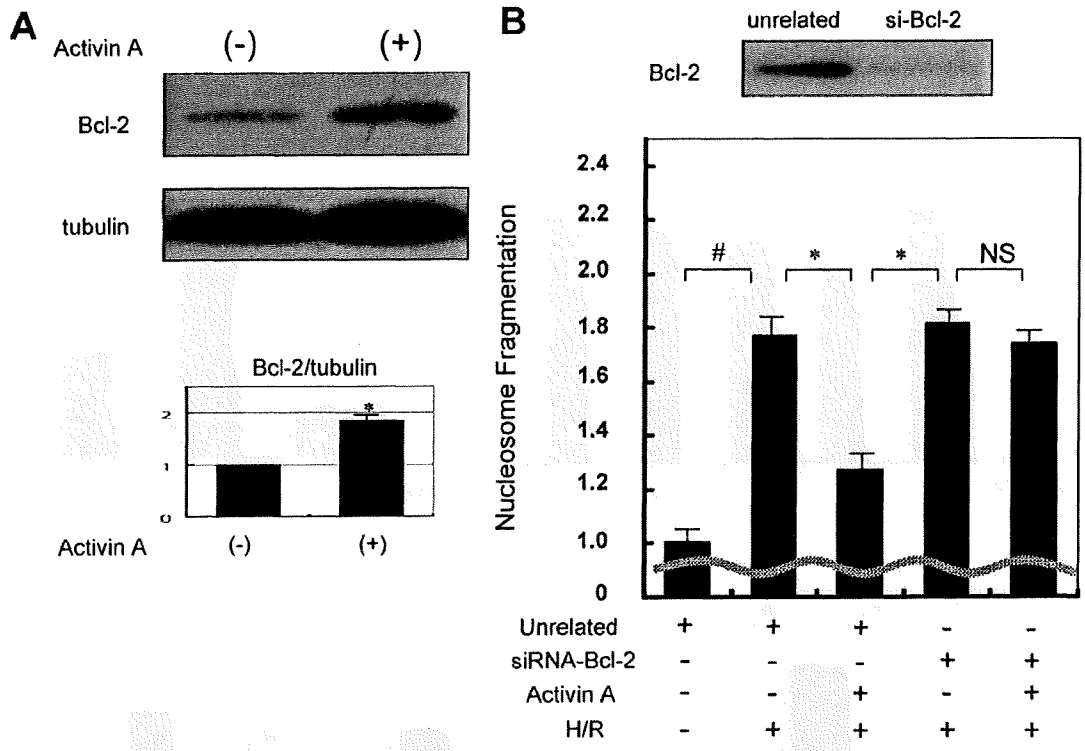

Figure 3. Cytoprotection by activin A is mediated by upregulation of the antiapoptotic protein Bcl-2. A, Activin A–induced Bcl-2 expression in NRVMs. A representative immunoblot is shown. Blots for α-tubulin were performed to indicate the equal loading. The histogram shows quantification of the band intensities to indicate a statistically significant increase in Bcl-2 protein expression after treatment with activin A. *$P<0.05$. B, Ablation of Bcl-2 expression blocks the cytoprotection conferred by activin A. The top panel shows a representative Western blot assessing the efficiency of siRNA targeting Bcl-2. The bottom panel displays the effect of Bcl-2 knockdown on activin A–mediated cytoprotection of NRVMs as determined by nucleosome fragmentation assay. Apoptosis was induced by H/R treatment. *$P<0.05$; #$P<0.01$.

cells (TOP10; Invitrogen) with the adenoviral backbone plasmid (pAdEasy-1). The recombinant adenoviral DNA with *Fstl3* or *activin βA* cDNA was extracted from the competent cells and transfected into HEK 293 cells to produce recombinant adenoviral vectors that express *Fstl3* (Ad-Fstl3) or *activin βA* (Ad-actβA). An adenoviral vector expressing β-galactosidase (Ad-βgal) was used as a control. The adenoviral vectors were purified by the CsCl ultracentrifugation method.

Adenovirus-Mediated Overexpression of Activin A in Mice

Eight- to 10-week-old male mice were injected intravenously with adenovirus (Ad-actβA or Ad-βgal; 5.0×10^9 plaque-forming units per mouse) through the jugular vein. Plasma activin A was assayed by Western blot analysis 3 days after adenovirus delivery. At this time point, mice also underwent myocardial ischemia/reperfusion (I/R) injury.

Generation of a Cardiac-Specific *Fstl3* Knockout Mice

Mice homozygous for an *Fstl3* allele with 2 *lox*P sites flanking exons 3 through 5 ($Fstl3^{flox/flox}$) were backcrossed and maintained on the C57BL6/J background. $Fstl3^{flox/flox}$ were crossed with α-myosin heavy chain (α-MHC)-Cre transgenic mice that are maintained on a C57BL6/J background. Four different primer pairs were used for genotyping polymerase chain reaction. The *lox*P site in intron 2 was detected with the use of the primer 1 (SJL954 TCTGAGAAGAGGAGGGATTTCAAG) and primer 2 (SJL955 ATTTACACCTAGCCACATACTCTG), which amplify an ≈390-bp fragment for the *lox*P site, whereas the *Fstl3* wild-type allele gives a 330-bp fragment. The *lox*P site in intron 5 was detected with the use of primer 3 (SJL956 AACCACATCCCAGATCCAGGTCAC) and primer 4 (SJL986 CAGCTATGTAGGCTTTGCATTGCTC), which amplify an ≈310-bp fragment for the *lox*P site and a 270-bp fragment for the wild-type allele. Recombination by Cre leads to an allele that lacks exons 3, 4, and 5 of the *Fstl3* gene and is detected with the use of primer pair of 1 and 4, which gives a 357-bp fragment. The α-MHC-Cre transgene is detected with the use of the primer pair of 5′-ATGACAGACAGATCCCTCCTATCTCC and 5′-CTCATCACTCGTTGCATCATCGAC, which amplifies a 300-bp fragment.

Statistical Analysis

Data are presented as mean±SEM. Group differences were analyzed by 2-tailed Student *t* test or ANOVA. To compare multiple groups, the Mann–Whitney *U* test with Bonferroni correction was used. A value of $P<0.05$ was considered statistically significant.

The authors had full access to and take full responsibility for the integrity of the data. All authors have read and agree to the manuscript as written.

Results

Activin βA and *Fstl3* Levels Are Regulated by Stress in the Heart

To better understand the roles of the TGF-β superfamily cytokines in heart, we analyzed transcript expression of family members by quantitative real-time polymerase chain reaction using cDNAs from mouse heart (Figure 1A). These analyses focused on *activin βA*, its inhibitory binding partners *follistatin* and *Fstl3*, and *inhibin α*. *Activin βA* showed marked upregulation at 1 and 3 days after left coronary artery

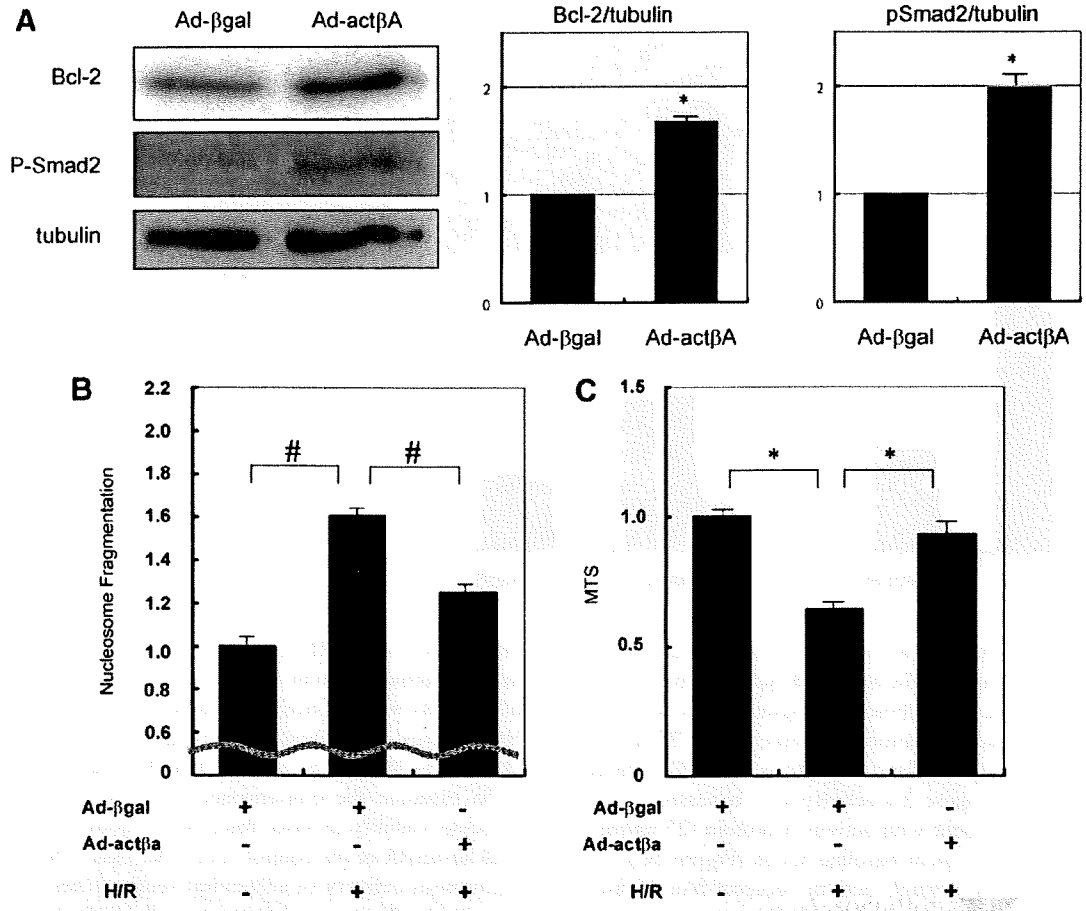

Figure 4. Adenovirus-encoded activin A induces Bcl-2 and protects cardiac myocytes from stress. A, Representative immunoblot images showing that transfection of adenoviral vector expressing *activin βA* (Ad-actβA) at an MOI of 50 resulted in increased expression of Bcl-2 and phosphorylation of Smad2. Membranes were blotted for α-tubulin to indicate equal protein loading. Histogram shows quantification of the band intensities. *$P<0.05$. Transduction of Ad-actβA (MOI=50) reduced apoptosis, assessed by the nucleosome fragmentation assay (B), and preserved cell viability, assessed by the MTS assay (C), against H/R stress. An adenovirus vector expressing β-galactosidase (Ad-βgal) was used as a control in these experiments at an MOI of 50. *$P<0.05$; #$P<0.01$.

ligation in the infarct zone and returned to baseline at the 6-day time point. These findings are in general agreement with those of Yndestad et al,[14] who previously reported a 15- to 40-fold induction of *activin βA* in the ischemic regions of heart after left coronary artery ligation in rats. *Fstl3* displayed statistically significant upregulation at days 1, 3, and 6 in the infarct and remote regions after left coronary artery ligation. *Follistatin* upregulation was observed in the infarct zone at the 3- and 6-day time points. No regulation of *inhibin* α, which opposes the action of *activin A*, was observed in this model.

Activin βA and *Fstl3* were upregulated 10- and 3-fold, respectively, after pressure overload at 1 week after transverse aortic constriction (Figure 1B), whereas the *follistatin* transcript level did not change, and the *inhibin* α transcript level declined by a factor of 2 (Figure 1B). In an I/R model, *Fstl3* expression was upregulated 4-fold at 12- and 24-hour time points after perfusion, whereas levels of *activin βA* increased 2-fold at the 12-hour time point (Figure 1C). Levels of *follistatin* and *inhibin* α did not change in these assays.

Dimers of activin βA are processed to give rise to the physiologically active protein activin A. Activin A levels were measured in hearts 3 days after left coronary artery ligation because the *activin βA* transcript was expressed robustly at this time point. A significant increase in activin A protein could be detected in hearts after infarction (Figure 1D). To document activin A and Fstl3 expression by cardiac myocytes, NRVMs were cultured under normoxic and H/R conditions (Figure 1E). Both proteins could be detected in lysates of the cell pellets and in the conditioned media. Treatment of cultures by H/R led to a 1.9-fold upregulation of activin A and a 1.7-fold upregulation of Fstl3 in the culture media ($P<0.05$; n=6).

Activin A Protects Cultured Myocytes From Apoptosis

In the noncardiac cell type, activin A has been reported to promote survival[15–17] or apoptosis.[18,19] Thus far, the effects of activin A on cardiac myocyte survival have not been reported. To elucidate the functional significance of activin A in cardiac myocytes, serum-deprived NRVMs were exposed to H/R stress in the presence or absence of recombinant human activin A protein and analyzed for markers of apoptotic cell death. As shown in Figure 2A, recombinant activin A protein promoted survival in NRVMs as assessed by an MTS assay. Statistically significant protection against apoptosis was observed when activin A was incubated with NRVMs at a dose

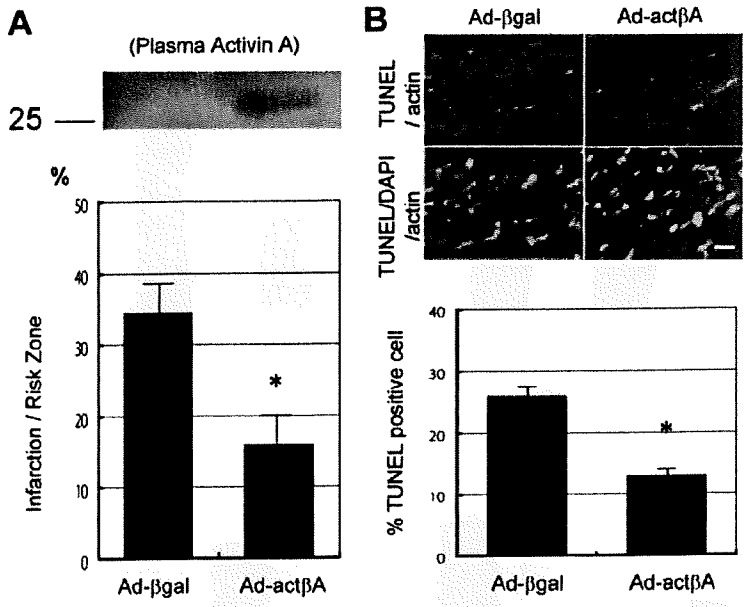

Figure 5. Adenovirus-mediated overexpression of activin A protects the heart from I/R injury. A, Representative Western blot analysis, performed under nonreducing conditions, of plasma samples collected 3 days after injection of Ad-βgal or Ad-actβA. Histogram shows quantification of infarct area induced by I/R 3 days after adenoviral injection. *$P<0.05$. B, Representative images of myocardium stained with TUNEL (green) and sarcomeric actin (red) (top panels) and merged with DAPI (blue) (bottom panels). Histogram shows quantification of TUNEL-positive cells in the myocardium after I/R. *$P<0.05$.

of 25 ng/mL. This level of activin A is similar to doses that exert antiapoptotic actions on other cell types.[20] To corroborate these findings, a nucleosome fragmentation assay of NRVM apoptosis was performed. Treatment with 25 ng/mL activin A reduced H/R-induced apoptosis by 62% (Figure 2B). Furthermore, caspase 3/7 activity was increased by the H/R stress, and treatment with activin A protein (25 ng/mL) reduced this activity to near baseline levels (Figure 2C).

Activin A signals through activin receptor-like kinases (ALKs).[1] Thus, NRVMs exposed to H/R stress were incubated with SB431542, a specific inhibitor of ALK4, ALK5, and ALK7, before treatment with recombinant activin A. Cell viability was assessed by MTS assay. As shown in Figure 2D, treatment with SB431542 abrogated the protective effect of activin A, whereas the inhibitor had no effect on basal cell viability. These data suggest that extracellular activin A protects cardiac myocytes from stress-induced apoptosis through the activities of ALKs.

To test whether Bcl-2 is involved in the antiapoptotic action of activin A in cardiac myocytes, Bcl-2 protein expression was determined by Western blot analysis. Activin A treatment significantly increased Bcl-2 protein levels in NRVMs (Figure 3A). Transduction of NRVMs with small interfering RNA (siRNA) targeting Bcl-2 reduced Bcl-2 protein expression. Knockdown of Bcl-2 with siRNA blocked the inhibitory effect of activin A on H/R-induced nucleosome fragmentation (Figure 3B). Thus, activin A cytoprotection is mediated by induction of Bcl-2.

Adenovirus-Mediated Expression of Activin A Promotes Myocyte Survival In Vitro and In Vivo

To corroborate and extend the findings obtained with the recombinant human activin A protein, an adenoviral vector that expresses the mouse *activin βA* gene (Ad-actβA) was generated. As shown in Figure 4A, transduction with Ad-actβA promoted the expression of Bcl-2 protein and increased the phosphorylation of Smad2 in NRVMs. The magnitude of these effects was similar to that observed with the recombinant activin A protein (Figure 3A). Transduction of NRVMs with Ad-actβA suppressed apoptosis induced by H/R as assessed by a nucleosome fragmentation assay (Figure 4B) and an MTS assay of cell viability (Figure 4C).

To examine the consequences of activin A on cardiac myocyte viability in vivo, mice were injected intravenously with ad-actβA or the control vector Ad-βgal. This method of intravenous delivery of adenoviral vectors leads to transduction of the liver but not heart, and secreted adenovirus-encoded proteins can be detected in the serum.[10,21] Mice receiving Ad-actβA exhibited detectable activin A protein expression in serum as assessed by Western blot analysis (Figure 5A). In response to myocardial I/R injury, mice treated with Ad-actβA displayed a 53.7% reduction in infarct size. This reduction corresponded to a decrease in the number of terminal deoxynucleotidyl transferase–mediated dUTP nick-end labeling (TUNEL)–positive, apoptotic cells in the area at risk of the Ad-actβA–treated group (Figure 5B). Collectively, these data show that activin A protects myocytes from apoptosis in vitro and in vivo and that it minimizes damage from I/R injury in the heart.

Fstl3 Inhibits Activin A–Mediated Protection of NRVMs

An adenoviral vector expressing the mouse *Fstl3* gene (Ad-Fstl3) was constructed because this factor is also induced by myocardial injury (Figure 1A to 1C), and it functions as an extracellular binding partner of activin A. Transduction of NRVMs with Ad-Fstl3 abrogated the ability of activin A protein to induce Smad2 phosphorylation (Figure 6A). In contrast, adenovirus-mediated overexpression of Fstl1 had no effect on activin A–induced Smad2 phosphorylation in NRVMs (Figure 6B).

Because Fstl3 is an inhibitor of activin A, we examined the effects of adeno-mediated induction of Fstl3 on activin A–mediated protection of NRVMs from stress-induced apoptosis. As

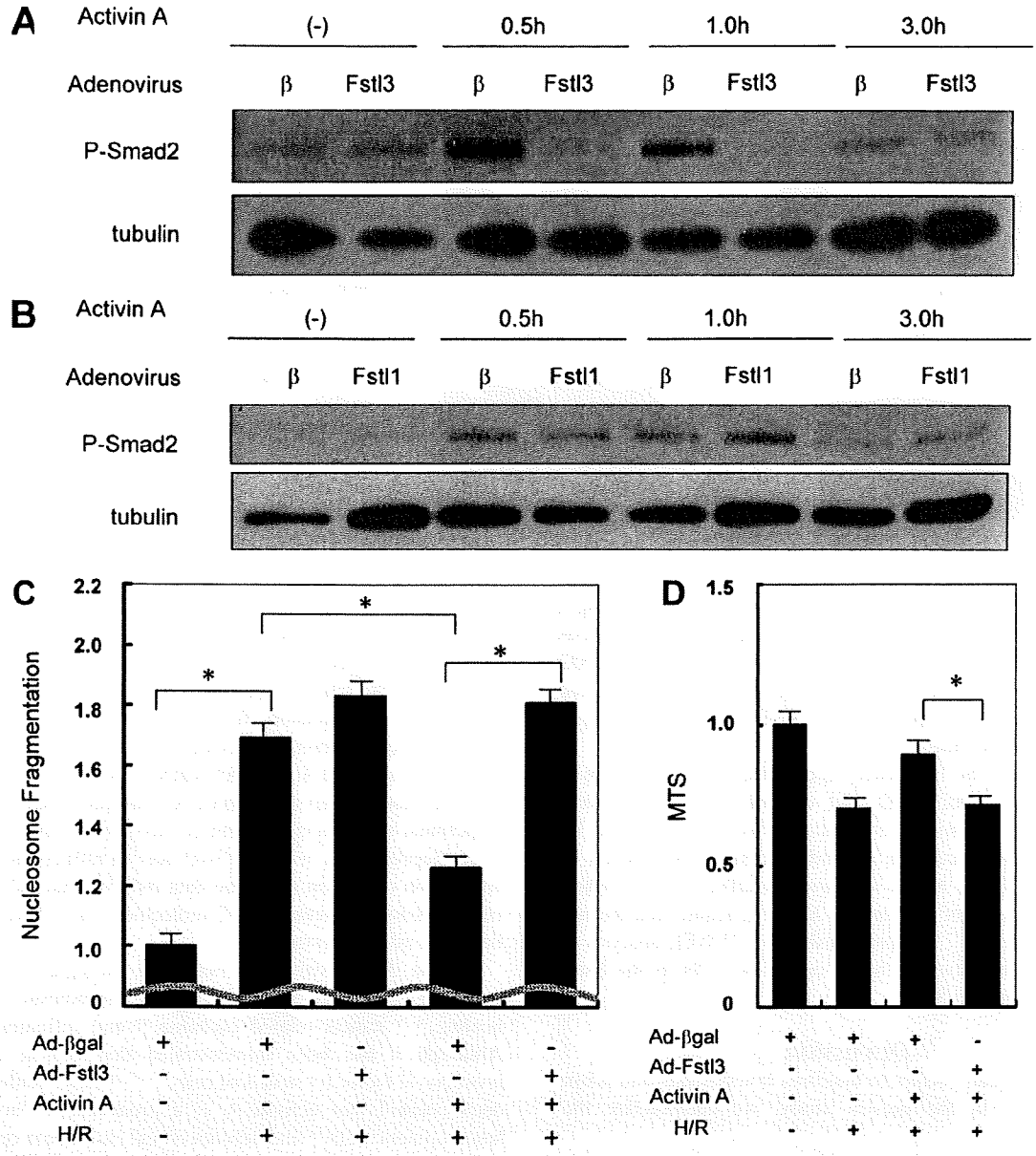

Figure 6. Fstl3 inhibits activin A action in NRVMs. A and B, NRVMs, transduced with Ad-Fstl3, Ad-Fstl1 or Ad-βgal (β) at 50 MOI, were stimulated with 25 ng/mL of recombinant activin A for indicated periods of time, and phosphorylation of Smad2 was determined by Western blot analysis. Immunoblots for α-tubulin were performed as a loading control. C and D, NRVMs were transduced with Ad-Fstl3 or Ad-βgal at an MOI of 50 (C) or 10 (D) and exposed to H/R treatment in the presence or absence of pretreatment with 25 ng/mL of activin A. Apoptosis was examined by nucleosome fragmentation assay (C), and cell viability was assessed by the MTS assay (D). *$P<0.05$.

shown by nucleosome fragmentation assay, transduction of Ad-Fstl3 abolished the prosurvival actions of activin A on NRVMs exposed to H/R stress (Figure 6C). The ability of Ad-Fstl3 to block activin A–mediated NRVM survival was corroborated by the MTS cell viability assay (Figure 6D).

Ablation of *Fstl3* in Cardiac Myocytes Protects the Heart From I/R Injury In Vivo

Cardiac myocyte–specific knockout mice for *Fstl3* were generated by crossing $Fstl3^{flox/flox}$ mice with mice expressing Cre recombinase from the α-MHC promoter. Cre-mediated recombination of the *Fstl3* allele in the hearts of α-MHC-Cre×$Fstl3^{flox/flox}$ (CKO) mice was confirmed by polymerase chain reaction (Figure I in the online-only Data Supplement). Quantitative real-time polymerase chain reaction analysis on the extracts from whole heart revealed a significant but incomplete reduction of *Fstl3* expression in CKO mice (Cre-f/f) compared with wild-type (W-f/f) mice (Figure 7A). Thus, cardiac myocytes were isolated from adult hearts of both strains of mice and evaluated for *Fstl3* expression (Figure 7B). Myocytes isolated from CKO mice were completely void of *Fstl3* transcript. Because whole-body *Fstl3*-deficient mice exhibit mild cardiac hypertrophy,[22] we evaluated the ratio of heart weight to body weight in the 2 strains

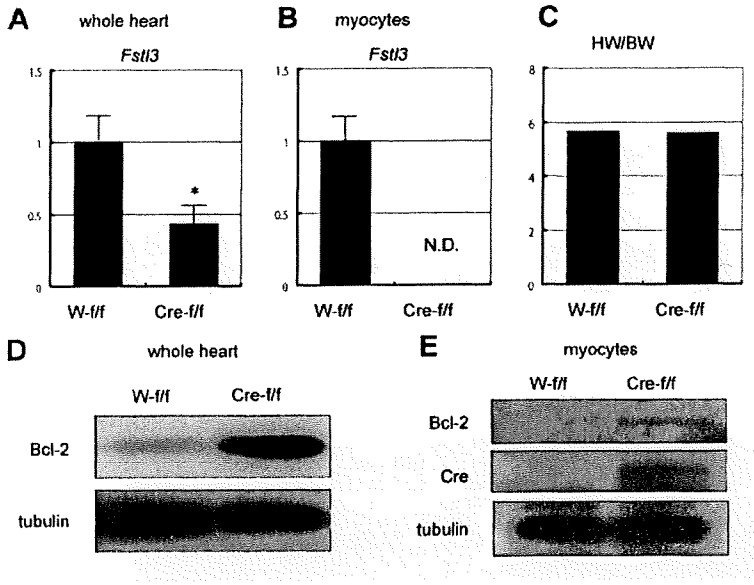

Figure 7. Fstl3 ablation in heart. A and B, Quantitative real-time polymerase chain reaction was performed to evaluate *Fslt3* mRNA expression in hearts of wild-type (W) or α-MHC-Cre (Cre) mice crossed with Fstl3$^{flox/flox}$ mice with the use of cDNA produced from whole heart extracts (A) or isolated cardiac myocytes (B). *$P<0.05$. C, Heart weight/body weight ratio (HW/BW) in 8-week-old male mice. D and E, Representative images of immunoblots of Bcl-2 expression in whole heart lysates (D) and isolated adult mouse cardiac myocytes (E). Immunoblots for α-tubulin are shown as a loading control.

of mice (Figure 7C). Cardiac myocyte–specific Fstl3 knockout mice did not show any difference in heart weight compared with wild-type mice. Western immunoblot analysis revealed the upregulation of Bcl-2 protein expression in CKO mice. The upregulation of Bcl-2 expression was also detected by Western immunoblot analysis of isolated cardiac myocytes from CKO hearts.

To examine the functional significance of *Fstl3* in myocytes of the heart, CKO and control mice hearts were subjected to I/R injury, and infarct size was analyzed by 2,3,5-triphenyltetrazolium chloride staining. As shown in Figure 8A, CKO hearts displayed smaller infarct zones, whereas the ratio of risk area to left ventricular area did not differ between the 2 groups (not shown). TUNEL analysis of the area at risk revealed fewer apoptotic cells in the Fstl3 CKO mice (Figure 8B).

Discussion

The heart secretes factors to maintain homeostasis and adapt to stress.[23–25] In the present study, we characterize the function of 2 new members of the cardiac secretome, Fstl3 and activin A. Fstl3 binds to activin A and other members of this family and inhibits their ability to activate signaling within target cells.[1] It has been reported that serum activin A levels and *Fstl3* transcript levels are elevated in heart failure,[9,14] but the regulatory functions of these factors in heart have not been examined previously. In this study, we show that both *Fstl3* and *Activin βA* mRNA are markedly upregulated in mouse heart in response to multiple types of injury. Functional analyses in vivo and in vitro showed that activin A is cardioprotective, whereas Fstl3 acts to nullify the protective action of activin A. These data indicate that the balance of expression between these 2 molecules can influence how the heart adapts to stress.

Activin A is involved in numerous biological processes including embryonic development,[26] erythropoiesis,[27] wound healing,[28,29] cancer-related cachexia,[30] and inflammation.[31] Although it has been demonstrated that activin A is a prosurvival factor for neuronal cells,[15–17,20] other studies have demonstrated that activin A is a proapoptotic factor for hematopoietic cells[18] and adrenocortical carcinoma cells.[19] It has also been reported that inhibition of activin A by follistatin attenuates apoptosis induced by carbon tetrachloride injury in liver.[32] Thus, the mode of activin A action is highly dependent on tissue and cell type. In the present study, we present multiple lines of evidence showing that activin A is cardioprotective. In cultured cardiac myocytes subjected to stress, treatment with recombinant activin A protein upregulated Bcl-2 protein expression and reduced caspase activation and cellular apoptosis. Consistent with these results, adenovirus-mediated activin A overexpression promoted Bcl-2 expression and myocyte viability. Adenovirus-mediated expression of activin A also reduced infarct size and the frequency of TUNEL-positive cells in hearts that underwent I/R injury.

The functional significance of Bcl-2 induction by activin A was assessed by siRNA knockdown experiments in vitro. Treatment with siRNA directed at Bcl-2 effectively ablated activin A–stimulated expression of this protein by cultured

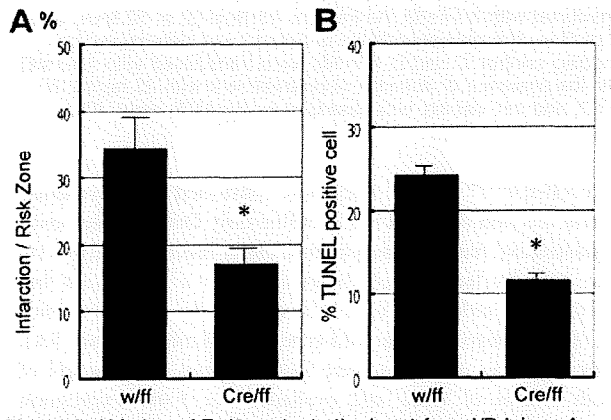

Figure 8. Ablation of Fstl3 protects the heart from I/R injury. A, Quantification of infarction size of *Fstl3*$^{flox/flox}$ crossed with wild-type (W/ff) or α-MHC-Cre (Cre/ff) after I/R injury. *$P<0.05$. B, Quantification of TUNEL-positive cells in the myocardium or control (W/ff) and CKO (Cre/ff) mice after I/R injury. *$P<0.05$.

myocytes and blocked the cytoprotection actions of activin A. Previous studies have shown that Bcl-2 has roles in promoting cardiac myocyte viability in models of ischemic injury[33] and desmin deficiency–induced cardiomyopathy.[34] It has also been reported that activin A induces both Bcl-2 and Bcl-xL in neuroblastoma and pheochromocytoma cells.[20] However, we did not detect activin A–stimulated Bcl-xL expression in cardiac myocyte cultures (data not shown).

In this study, it is shown that Fstl3 inhibits the protective actions of activin A on cardiac myocytes. Pretreatment with an adenoviral vector expressing Fstl3 abrogates activin A–mediated suppression of NRVM death under conditions of H/R. Furthermore, cardiac myocyte–specific ablation of Fslt3 reduces infarct size and diminishes the frequency of apoptotic myocytes in the area at risk after I/R injury.

We previously showed that Fstl1 is upregulated by cardiac injuries in murine models,[10] and Lara-Pezzi et al reported that the *Fstl1* transcript is upregulated in human heart failure.[9] In contrast to Fstl3, Fstl1 protects cardiac myocytes from death both in vitro and in vivo.[10] Also in contrast to Fslt3, it is shown here that Fstl1 does not interfere with activin A–stimulated Smad2 phosphorylation (Figure 6). In contrast, Fstl1 protection of both cardiac myocytes and endothelial cells is dependent on the upregulation of Akt signaling.[10,35] Currently, there is no evidence to suggest that Fstl1 functions by binding to TGF-β superfamily members.

It was previously reported that whole-body *Fstl3* deficiency results in a low degree of cardiac hypertrophy accompanied by mildly elevated blood pressure in old female mice.[22] In the present study, we employed cardiac-specific Fstl3-deficient mice, and no change in ratio of heart weight to body weight was observed between CKO and wild-type mice. Because elevated blood pressure can lead to cardiac hypertrophy, the cardiac phenotype of the whole-body Fstl3 knockout mouse may be caused by the indirect actions of whole-body *Fstl3* deficiency on the heart.

Other TGF-β family cytokines reported to be produced by the heart under conditions of stress include myostatin/GDF-8 and GDF-15.[6–8,36] Like activin A, these factors regulate Smad signaling and cause cachexia when administered or overexpressed.[30,37,38] Both activin A and GDF-15 have been shown to be increased in patients with heart diseases.[14,39,40] Collectively, these studies indicate the existence of a broad signaling network involving TGF-β family factors and their extracellular inhibitory proteins that control cardiac adaptation to stress. The expression of these proteins by the damaged heart may also contribute to the systemic wasting response in chronic heart failure.

Conclusions

We show that activin A and its extracellular inhibitory protein Fstl3 are upregulated in murine heart under conditions of stress. Administration or overexpression of activin A protects myocytes from stress in vitro and in vivo. In contrast, Fstl3 overexpression inhibits the myocyte-protective activity of activin A in vitro, and cardiac-specific Fstl3-deficient mice display smaller infarcts and less myocyte apoptosis in response to I/R injury. Thus, we propose that activin A and Fstl3 function in an opposing manner to regulate myocyte survival and that the relative expression levels of these factors influence the adaptive response of the heart to injury.

Sources of Funding

This study was funded by National Institutes of Health grants HL77774, HL86785, AG15052, and HL81587 to K. Walsh. N. Ouchi was supported by American Heart Association grant 0635593T. D.R. Pimentel was supported by National Institutes of Health grant HL71563. Y. Oshima was supported by American Heart Association grant 0625867T. S. Lee was supported by National Institutes of Health grant U54-AR052646. K.D. Panse was supported by an EMBO fellowship (ASTF 53.00-2009).

Disclosures

None.

References

1. Shi Y, Massague J. Mechanisms of TGF-beta signaling from cell membrane to the nucleus. *Cell*. 2003;113:685–700.
2. Schultz Jel J, Witt SA, Glascock BJ, Nieman ML, Reiser PJ, Nix SL, Kimball TR, Doetschman T. TGF-beta1 mediates the hypertrophic cardiomyocyte growth induced by angiotensin II. *J Clin Invest*. 2002;109:787–796.
3. Okada H, Takemura G, Kosai K, Li Y, Takahashi T, Esaki M, Yuge K, Miyata S, Maruyama R, Mikami A, Minatoguchi S, Fujiwara T, Fujiwara H. Postinfarction gene therapy against transforming growth factor-beta signal modulates infarct tissue dynamics and attenuates left ventricular remodeling and heart failure. *Circulation*. 2005;111:2430–2437.
4. Izumi M, Fujio Y, Kunisada K, Negoro S, Tone E, Funamoto M, Osugi T, Oshima Y, Nakaoka Y, Kishimoto T, Yamauchi-Takihara K, Hirota H. Bone morphogenetic protein-2 inhibits serum deprivation-induced apoptosis of neonatal cardiac myocytes through activation of the Smad1 pathway. *J Biol Chem*. 2001;276:31133–31141.
5. Masaki M, Izumi M, Oshima Y, Nakaoka Y, Kuroda T, Kimura R, Sugiyama S, Terai K, Kitakaze M, Yamauchi-Takihara K, Kawase I, Hirota H. Smad1 protects cardiomyocytes from ischemia-reperfusion injury. *Circulation*. 2005;111:2752–2759.
6. Xu J, Kimball TR, Lorenz JN, Brown DA, Bauskin AR, Klevitsky R, Hewett TE, Breit SN, Molkentin JD. GDF15/MIC-1 functions as a protective and antihypertrophic factor released from the myocardium in association with SMAD protein activation. *Circ Res*. 2006;98:342–350.
7. Kempf T, Eden M, Strelau J, Naguib M, Willenbockel C, Tongers J, Heineke J, Kotlarz D, Xu J, Molkentin JD, Niessen HW, Drexler H, Wollert KC. The transforming growth factor-beta superfamily member growth-differentiation factor-15 protects the heart from ischemia/reperfusion injury. *Circ Res*. 2006;98:351–360.
8. Morissette MR, Cook SA, Foo S, McKoy G, Ashida N, Novikov M, Scherrer-Crosbie M, Li L, Matsui T, Brooks G, Rosenzweig A. Myostatin regulates cardiomyocyte growth through modulation of Akt signaling. *Circ Res*. 2006;99:15–24.
9. Lara-Pezzi E, Felkin LE, Birks EJ, Sarathchandra P, Panse KD, George R, Hall JL, Yacoub MH, Rosenthal N, Barton PJ. Expression of follistatin-related genes is altered in heart failure. *Endocrinology*. 2008:149:5822–5827.
10. Oshima Y, Ouchi N, Sato K, Izumiya Y, Pimentel DR, Walsh K. Follistatin-like 1 is an Akt-regulated cardioprotective factor that is secreted by the heart. *Circulation*. 2008;117:3099–3108.
11. Schiekofer S, Shiojima I, Sato K, Galasso G, Oshima Y, Walsh K. Microarray analysis of Akt1 activation in transgenic mouse hearts reveals transcript expression profiles associated with compensatory hypertrophy and failure. *Physiol Genomics*. 2006;27:156–170.
12. Schiekofer S, Belisle K, Galasso G, Schneider JG, Boehm BO, Burster T, Schmitz G, Walsh K. Angiogenic-regulatory network revealed by molecular profiling heart tissue following Akt1 induction in endothelial cells. *Angiogenesis*. 2008;11:289–299.
13. Shibata R, Sato K, Pimentel DR, Takemura Y, Kihara S, Ohashi K, Funahashi T, Ouchi N, Walsh K. Adiponectin protects against myocardial ischemia-reperfusion injury through AMPK- and COX-2-dependent mechanisms. *Nat Med*. 2005;11:1096–1103.
14. Yndestad A, Ueland T, Oie E, Florholmen G, Halvorsen B, Attramadal H, Simonsen S, Froland SS, Gullestad L, Christensen G, Damas JK, Aukrust

P. Elevated levels of activin A in heart failure: potential role in myocardial remodeling. *Circulation*. 2004;109:1379–1385.
15. Hughes PE, Alexi T, Williams CE, Clark RG, Gluckman PD. Administration of recombinant human activin-A has powerful neurotrophic effects on select striatal phenotypes in the quinolinic acid lesion model of Huntington's disease. *Neuroscience*. 1999;92:197–209.
16. Wu DD, Lai M, Hughes PE, Sirimanne E, Gluckman PD, Williams CE. Expression of the activin axis and neuronal rescue effects of recombinant activin A following hypoxic-ischemic brain injury in the infant rat. *Brain Res*. 1999;835:369–378.
17. Schubert D, Kimura H, LaCorbiere M, Vaughan J, Karr D, Fischer WH. Activin is a nerve cell survival molecule. *Nature*. 1990;344:868–870.
18. Valderrama-Carvajal H, Cocolakis E, Lacerte A, Lee EH, Krystal G, Ali S, Lebrun JJ. Activin/TGF-beta induce apoptosis through Smad-dependent expression of the lipid phosphatase SHIP. *Nat Cell Biol*. 2002;4:963–969.
19. Vanttinen T, Liu J, Kuulasmaa T, Kivinen P, Voutilainen R. Expression of activin/inhibin signaling components in the human adrenal gland and the effects of activins and inhibins on adrenocortical steroidogenesis and apoptosis. *J Endocrinol*. 2003;178:479–489.
20. Kupershmidt L, Amit T, Bar-Am O, Youdim MB, Blumenfeld Z. The neuroprotective effect of Activin A and B: implication for neurodegenerative diseases. *J Neurochem*. 2007;103:962–971.
21. Shibata R, Sato K, Kumada M, Izumiya Y, Sonoda M, Kihara S, Ouchi N, Walsh K. Adiponectin accumulates in myocardial tissue that has been damaged by ischemia-reperfusion injury via leakage from the vascular compartment. *Cardiovasc Res*. 2007;74:471–479.
22. Mukherjee A, Sidis Y, Mahan A, Raher MJ, Xia Y, Rosen ED, Bloch KD, Thomas MK, Schneyer AL. FSTL3 deletion reveals roles for TGF-beta family ligands in glucose and fat homeostasis in adults. *Proc Natl Acad Sci U S A*. 2007;104:1348–1353.
23. Shiojima I, Sato K, Izumiya Y, Schiekofer S, Ito M, Liao R, Colucci WS, Walsh K. Disruption of coordinated cardiac hypertrophy and angiogenesis contributes to the transition to heart failure. *J Clin Invest*. 2005;115:2108–2118.
24. Frost RJ, Engelhardt S. A secretion trap screen in yeast identifies protease inhibitor 16 as a novel antihypertrophic protein secreted from the heart. *Circulation*. 2007;116:1768–1775.
25. Izumiya Y, Shiojima I, Sato K, Sawyer DB, Colucci WS, Walsh K. Vascular endothelial growth factor blockade promotes the transition from compensatory cardiac hypertrophy to failure in response to pressure overload. *Hypertension*. 2006;47:887–893.
26. Matzuk MM, Kumar TR, Vassalli A, Bickenbach JR, Roop DR, Jaenisch R, Bradley A. Functional analysis of activins during mammalian development. *Nature*. 1995;374:354–356.
27. Murata M, Eto Y, Shibai H, Sakai M, Muramatsu M. Erythroid differentiation factor is encoded by the same mRNA as that of the inhibin beta A chain. *Proc Natl Acad Sci U S A*. 1988;85:2434–2438.
28. Munz B, Smola H, Engelhardt F, Bleuel K, Brauchle M, Lein I, Evans LW, Huylebroeck D, Balling R, Werner S. Overexpression of activin A in the skin of transgenic mice reveals new activities of activin in epidermal morphogenesis, dermal fibrosis and wound repair. *EMBO J*. 1999;18:5205–5215.
29. Wankell M, Munz B, Hubner G, Hans W, Wolf E, Goppelt A, Werner S. Impaired wound healing in transgenic mice overexpressing the activin antagonist follistatin in the epidermis. *EMBO J*. 2001;20:5361–5372.
30. Matzuk MM, Finegold MJ, Mather JP, Krummen L, Lu H, Bradley A. Development of cancer cachexia-like syndrome and adrenal tumors in inhibin-deficient mice. *Proc Natl Acad Sci U S A*. 1994;91:8817–8821.
31. Jones KL, Mansell A, Patella S, Scott BJ, Hedger MP, de Kretser DM, Phillips DJ. Activin A is a critical component of the inflammatory response, and its binding protein, follistatin, reduces mortality in endotoxemia. *Proc Natl Acad Sci U S A*. 2007;104:16239–16244.
32. Patella S, Phillips DJ, Tchongue J, de Kretser DM, Sievert W. Follistatin attenuates early liver fibrosis: effects on hepatic stellate cell activation and hepatocyte apoptosis. *Am J Physiol*. 2006;290:G137–G144.
33. Imahashi K, Schneider MD, Steenbergen C, Murphy E. Transgenic expression of Bcl-2 modulates energy metabolism, prevents cytosolic acidification during ischemia, and reduces ischemia/reperfusion injury. *Circ Res*. 2004;95:734–741.
34. Weisleder N, Taffet GE, Capetanaki Y. Bcl-2 overexpression corrects mitochondrial defects and ameliorates inherited desmin null cardiomyopathy. *Proc Natl Acad Sci U S A*. 2004;101:769–774.
35. Ouchi N, Oshima Y, Ohashi K, Higuchi A, Ikegami C, Izumiya Y, Walsh K. Follistatin-like 1, a secreted muscle protein, promotes endothelial cell function and revascularization in ischemic tissue through a nitric-oxide synthase-dependent mechanism. *J Biol Chem*. 2008;283:32802–32811.
36. Sharma M, Kambadur R, Matthews KG, Somers WG, Devlin GP, Conaglen JV, Fowke PJ, Bass JJ. Myostatin, a transforming growth factor-beta superfamily member, is expressed in heart muscle and is upregulated in cardiomyocytes after infarct. *J Cell Physiol*. 1999;180:1–9.
37. Zimmers TA, Davies MV, Koniaris LG, Haynes P, Esquela AF, Tomkinson KN, McPherron AC, Wolfman NM, Lee SJ. Induction of cachexia in mice by systemically administered myostatin. *Science*. 2002;296:1486–1488.
38. Johnen H, Lin S, Kuffner T, Brown DA, Tsai VW, Bauskin AR, Wu L, Pankhurst G, Jiang L, Junankar S, Hunter M, Fairlie WD, Lee NJ, Enriquez RF, Baldock PA, Corey E, Apple FS, Murakami MM, Lin EJ, Wang C, During MJ, Sainsbury A, Herzog H, Breit SN. Tumor-induced anorexia and weight loss are mediated by the TGF-beta superfamily cytokine MIC-1. *Nat Med*. 2007;13:1333–1340.
39. Kempf T, von Haehling S, Peter T, Allhoff T, Cicoira M, Doehner W, Ponikowski P, Filippatos GS, Rozentryt P, Drexler H, Anker SD, Wollert KC. Prognostic utility of growth differentiation factor-15 in patients with chronic heart failure. *J Am Coll Cardiol*. 2007;50:1054–1060.
40. Wollert KC, Kempf T, Peter T, Olofsson S, James S, Johnston N, Lindahl B, Horn-Wichmann R, Brabant G, Simoons ML, Armstrong PW, Califf RM, Drexler H, Wallentin L. Prognostic value of growth-differentiation factor-15 in patients with non-ST-elevation acute coronary syndrome. *Circulation*. 2007;115:962–971.

CLINICAL PERSPECTIVE

The injured heart secretes proteins that influence its function. In this study, we characterize 2 new members of the cardiac "secretome," activin A and follistatin-like 3 (Fstl3), using genetic gain- and loss-of-function manipulations in mouse models. Activin A and Fstl3 expression was increased in heart after various injuries and in cultured myocytes after hypoxia/reoxygenation. Activin A protected myocytes from cell death, and this protective activity was antagonized by Fstl3, which functions as an extracellular inhibitory protein for activin A. Myocardial ischemia/reperfusion injury was reduced in mice administered activin A. Genetic ablation of Fstl3 in cardiac myocytes also diminished injury in response to ischemia/reperfusion. We speculate that activin A and Fstl3 serve as sensors of cardiac stress and that their relative levels of expression influence the adaptive response of the heart to injury.

nature
cell biology

Mesenchymal progenitors distinct from satellite cells contribute to ectopic fat cell formation in skeletal muscle

Akiyoshi Uezumi[1,5], So-ichiro Fukada[2], Naoki Yamamoto[3], Shin'ichi Takeda[4] and Kunihiro Tsuchida[1]

Ectopic fat deposition in skeletal muscle is closely associated with several disorders, however, the origin of these adipocytes is not clear, nor is the mechanism of their formation. Satellite cells function as adult muscle stem cells but are proposed to possess multipotency. Here, we identify PDGFRα$^+$ mesenchymal progenitors as being distinct from satellite cells and located in the muscle interstitium. We show that, of the muscle-derived cell populations, only PDGFRα$^+$ cells show efficient adipogenic differentiation both *in vitro* and *in vivo*. Reciprocal transplantation between regenerating and degenerating muscles, and co-culture experiments revealed that adipogenesis of PDGFRα$^+$ cells is strongly inhibited by the presence of satellite cell-derived myofibres. These results suggest that PDGFRα$^+$ mesenchymal progenitors are the major contributor to ectopic fat cell formation in skeletal muscle, and emphasize that interaction between muscle cells and PDGFRα$^+$ mesenchymal progenitors, not the fate decision of satellite cells, has a considerable impact on muscle homeostasis.

Adult skeletal muscle possesses a remarkable regenerative ability. This depends on satellite cells that reside adjacent to and beneath the basal lamina of myofibres and function as adult muscle stem cells[1]. Despite that, in several pathological conditions where muscle integrity has been debilitated, skeletal muscle is occupied by adipocytes. The most striking accumulation of adipocytes is seen in advanced cases of Duchenne muscular dystrophy (DMD), where a muscle may be almost entirely replaced by adipocytes[2]. However, fat accumulation can be seen not only in myopathies but also in severe neurogenic atrophy, type II diabetes, obesity or ageing-related sarcopenia[3–6]. Nevertheless, the precise origin of ectopic adipocytes is not clear, and nor is the stimulus that incites their formation.

Adipose cells are thought to be derived from mesenchymal stem cells (MSCs). During adipose tissue development, MSCs commit into adipocyte lineage and eventually give rise to preadipocytes, which cannot be distinguished from MSCs by their morphology or gene expression, but have lost potential for differentiation to other cell lineages[7]. Preadipocytes then undergo terminal differentiation that involves a highly regulated and coordinated cascade of transcription factors[8]. C/EBPα and PPARγ are the best-characterized transcriptional factors for adipogenesis[9,10]. These two factors function cooperatively to transactivate adipocyte genes and continue to be expressed in mature adipocytes. Lineage commitment and differentiation of adipose progenitors or stem cells should occur in ectopic fat formation in skeletal muscle as well as in adipose tissue development. Several types of cell isolated from skeletal muscle have been reported to possess adipogenic differentiation potential including satellite cells[11,12], side population cells[13] and MSCs[14,15]. However, it is not clear whether these cells have the ability to induce *in vivo* fat formation in skeletal muscle. It is not known whether satellite cell plasticity or multipotency is operative *in vivo*, and little is known about the *in vivo* features of muscle side population cells or MSCs, such as their anatomical localization and pathophysiological roles.

Here, we conducted a comprehensive analysis of cells that reside in skeletal muscle to clarify the origin of the cell population that is involved in adipogenesis in this muscle type.

RESULTS

In vitro adipogenic potential is detected only in the PDGFRα$^+$ mesenchymal progenitor population of muscle-derived cells

We first fractionated whole mononucleated cells, which had been enzymatically isolated from skeletal muscle, based on the expression of established cell surface markers: CD31 as an endothelial marker, CD45 as a pan-haematopoietic marker and SM/C-2.6 as a marker of satellite cells (Fig. 1a)[16]. After sorting by fluorescence activated cell sorting (FACS), each cell population was cultured under adipogenic conditions to compare their adipogenic potentials (Fig. 1b). Oil red O staining revealed that only CD31$^-$CD45$^-$SM/C-2.6$^-$ cells efficiently differentiated into adipocytes (Fig. 1c). Freshly isolated CD31$^-$CD45$^-$SM/C-2.6$^-$ cells did not express endothelial, haematopoietic and myogenic genes; however, they did express *PDGFRα* and *PDGFRβ*, which have been shown to be present in mesenchymal cells (Fig. 1d)[17,18]. In particular, strong expression of *PDGFRα* was detected. When whole muscle-derived cells were fractionated on the basis of CD31,

[1]Division for Therapies against Intractable Diseases, Institute for Comprehensive Medical Science, Fujita Health University, 1-98 Dengakugakubo, Kutsukake, Toyoake, Aichi 470-1192, Japan. [2]Department of Immunology, Graduate School of Pharmaceutical Sciences, Osaka University, 1-6 Yamada-oka, Suita, Osaka 565-0871, Japan. [3]Laboratory of Molecular Biology & Histochemistry, Fujita Health University Joint Research Laboratory, Aichi 470-1192, Japan. [4]Department of Molecular Therapy, National Institute of Neuroscience, National Center of Neurology and Psychiatry (NCNP), 4-1-1 Ogawa-higashi, Kodaira, Tokyo 187-8502, Japan. [5]Correspondence should be addressed to A.U. (e-mail: uezumi@fujita-hu.ac.jp).

Received 20 May 2009; accepted 23 November 2009; published online 17 January 2010; DOI: 10.1038/ncb2014

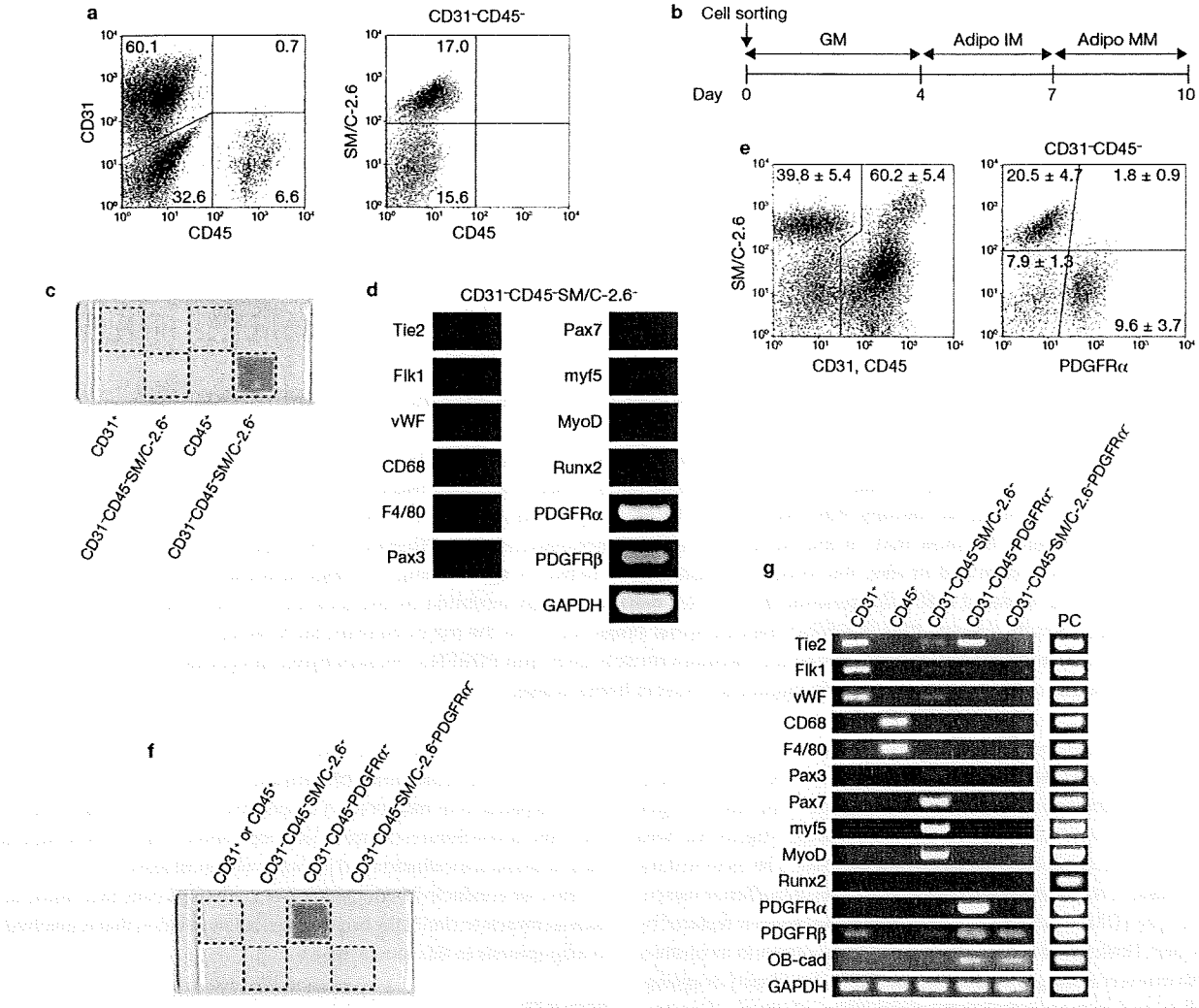

Figure 1 *In vitro* adipogenic potential was found only in the PDGFRα⁺ population of muscle-derived cells. **(a)** Whole muscle-derived cells were analysed for CD31, CD45 and SM/C-2.6 expression by flow cytometry. The percentages of each cell population are shown in the panels and expressed as the mean of three independent experiments. **(b)** Protocol for *in vitro* adipogenic differentiation. Freshly sorted cells were cultured in growth medium (GM) for 4 days before treatment with adipogenic induction medium (Adipo IM) for 3 days and treatment with adipogenic maintenance medium (Adipo MM) for 3 days. **(c)** Whole muscle-derived cells were divided into the four fractions indicated. Each fraction was cultured and induced to differentiate into adipocytes. A macroscopic view of an oil red O-stained eight-well chamber slide is shown. **(d)** RT-PCR analysis of lineage markers in freshly isolated CD31⁻CD45⁻SM/C-2.6⁻ cells. **(e)** Whole muscle-derived cells were analysed for CD31, CD45, SM/C-2.6 and PDGFRα expression. The percentages of each cell population are expressed as the mean ± s.d. of ten independent experiments. **(f)** The four fractions indicated were purified from gross muscle-derived mononucleated cells and cultured under adipogenic conditions. A macroscopic view of the oil red O stained eight-well chamber slide is shown. **(g)** Expression of lineage markers in the five fractions indicated. RNA was extracted from freshly isolated cells immediately after cell sorting and RT-PCR was performed. RNA extracted from whole embryos at embryonic day (E) 13.5 was used as a positive control (PC).

CD45, SM/C-2.6 and PDGFRα expression and induced to differentiate into adipocytes, adipogenic activity was detected only in PDGFRα⁺ cells (Fig. 1e, f). Reverse transcription-PCR (RT-PCR) analysis of freshly isolated cells showed that *PDGFRα* was specifically detected in PDGFRα⁺ cells, indicating specific expression of this molecule at both the mRNA and protein levels (Fig. 1g). In addition to the expression of mesenchymal genes, there was observable expression of the *Tie2* gene in PDGFRα⁺ cells (Fig. 1g). Tie2 has been reported to identify mesenchymal progenitors in addition to endothelial cells and a subset of haematopoietic cells[19]. Phenotypic analysis of freshly isolated PDGFRα⁺ cells revealed that they are similar to MSCs with respect to their surface phenotypes (Supplementary Information, Fig. S1a). Absence of Pax7 and adipogenic transcription factors indicated that satellite cells and committed adipogenic cells were not included in the PDGFRα⁺ fraction (Supplementary Information, Fig. S1b, c).

We next investigated *in vitro* adipogenesis of muscle-derived cell populations. Although a mixed population of CD31⁺ and CD45⁺ cells or a population of CD31⁻CD45⁻SM/C-2.6⁻PDGFRα⁻ cells proliferated poorly, two other populations, CD31⁻CD45⁻PDGFRα⁺ and CD31⁻CD45⁻SM/C-2.6⁺, proliferated actively (Fig. 2a). CD31⁻CD45⁻SM/C-2.6⁺ cells were negative for PDGFRα, C/EBPα and PPARγ (Fig. 2b), but almost all of these cells expressed Pax7 and MyoD, and a few were positive for myogenin on day 4 (Supplementary Information, Fig. S2a, d). Even upon adipogenic

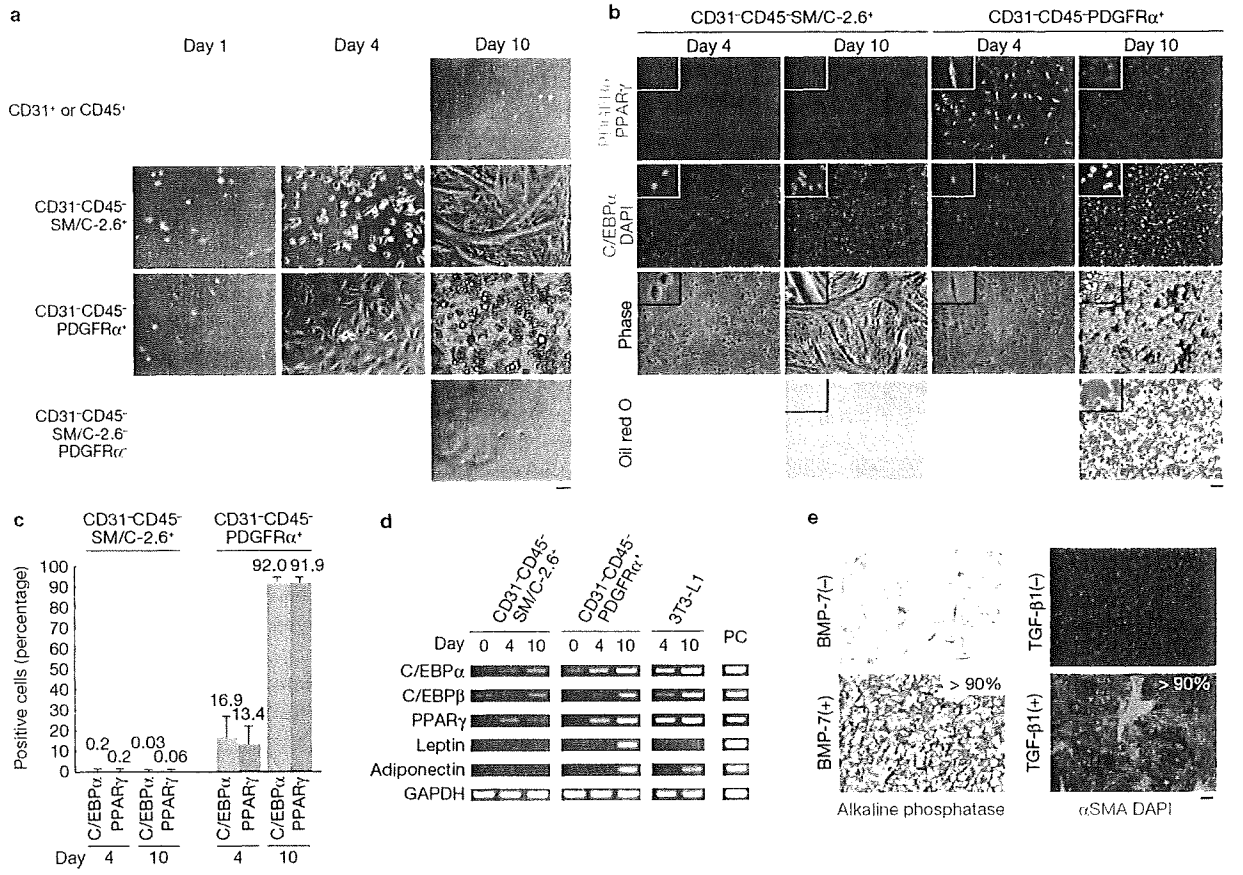

Figure 2 *In vitro* adipogenesis of muscle-derived cells. **(a)** Phase contrast images of a mixed population of CD31$^+$ and CD45$^+$ cells, CD31$^-$CD45$^-$ SM/C-2.6$^+$ cells, CD31$^-$CD45$^-$PDGFRα$^+$ cells and CD31$^-$CD45$^-$SM/C-2.6$^-$ PDGFRα$^-$ cells under adipogenic culture conditions. **(b)** Cultured CD31$^-$ CD45$^-$SM/C-2.6$^+$ cells and CD31$^-$CD45$^-$PDGFRα$^+$ cells were fixed at the time points indicated and stained with antibodies against PDGFRα, C/EBPα and PPARγ, or with oil red O. Insets show high magnification images. **(c)** Adipogenic differentiation was evaluated by quantifying the percentages of C/EBPα- and PPARγ-positive cells. Error bars indicate mean ± s.d., $n = 15$ fields pulled out from three independent experiments. **(d)** Expression of adipogenic genes in CD31$^-$CD45$^-$SM/C-2.6$^+$ cells, CD31$^-$ CD45$^-$PDGFRα$^+$ cells and 3T3-L1 cells during adipogenic culture. PC, positive control. **(e)** Multi-lineage differentiation of CD31$^-$CD45$^-$PDGFRα$^+$ cells. These cells were treated with BMP-7 or TGF-β1, and then alkaline phosphatase activity and αSMA expression were examined. The values in the bottom panels represent the percentages of positive cells. Scale bars, 50 μm (**a**, **b**, **e**).

induction, they did not differentiate into adipocytes, but instead differentiated into well-developed large myotubes (Fig. 2b, c; Supplementary Information, Fig. S2b). In contrast, CD31$^-$CD45$^-$PDGFRα$^+$ cells had maintained PDGFRα expression, and began to express C/EBPα and PPARγ on day 4 (Fig. 2b), but they did not express myogenic markers (Supplementary Information, Fig. S2c, d). Upon adipogenic induction, over 90% of CD31$^-$CD45$^-$PDGFRα$^+$ cells differentiated into adipocytes, adopting a spherical shape, accumulating lipid and expressing C/EBPα and PPARγ (Fig. 2b, c). A clonal assay revealed that nearly 80% of clones were adipogenic (Supplementary Information, Fig. S3). After adipogenic differentiation, these cells were no longer positive for PDGFRα (Fig. 2b). PDGFRα$^+$ cell-derived adipocytes expressed much higher levels of *leptin* compared with adipocytes derived from 3T3-L1 preadipocytes, although this was lower than that of *in vivo* white adipose tissue (Fig. 2d; Supplementary Information, Fig. S4). Similar results were obtained when each muscle-derived cell population was cultured directly in adipogenic induction medium immediately after cell sorting (Supplementary Information, Fig. S5). In addition to adipogenic potential, these cells readily differentiated into osteoblastic and smooth muscle-like cells with high efficiency under specific culture conditions (Fig. 2e; Supplementary Information, Fig. S6), but scarcely differentiated into skeletal muscle cells when cultured under myogenic differentiation conditions or transplanted into regenerating muscle (data not shown; Supplementary Information, Fig. S7). The high efficiency of differentiation into three different cell types strongly suggests that muscle-derived PDGFRα$^+$ cells populations are highly enriched for mesenchymal progenitors.

Localization of PDGFRα$^+$ cells in skeletal muscle

Next, we examined the anatomical localization of PDGFRα$^+$ cells in skeletal muscle. PDGFRα$^+$ cells were localized at the interstitial space of muscle tissue, whereas satellite cells (stained with Pax7 or M-cadherin, M-cad, antibodies) were located beneath the basement membrane (Fig. 3a; Supplementary Information, Fig. S8a). These localizations again indicate that PDGFRα$^+$ cells and satellite cells represent discrete cell populations. The mesenchymal origin of the PDGFRα$^+$ cells was supported by the expression of the mesenchymal intermediate filament, Vimentin (Fig. 3b). These cells also express a known repressor of adipogenesis, Dlk1 (also known as Pref-1; Supplementary Information, Fig. S8b). As pericytes have been reported

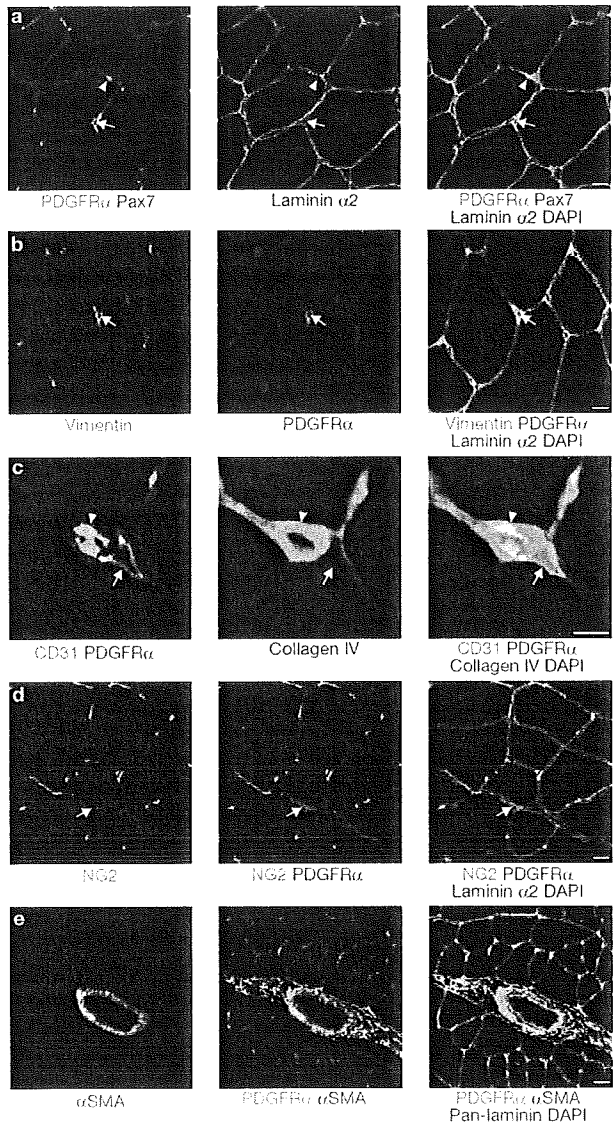

Figure 3 Localization of PDGFRα⁺ cells in adult skeletal muscle. **(a–e)** Tibialis anterior or gastrocnemius muscle sections were stained with antibodies against PDGFRα, Pax7 and laminin α2 **(a)**; Vimentin, PDGFRα and laminin α2 **(b)**; CD31, PDGFRα and collagen IV **(c)**; NG2, PDGFRα and laminin α2 **(d)** or αSMA, PDGFRα and pan-laminin **(e)**. Arrows indicate PDGFRα⁺ cells located in the interstitial space of muscle tissue. Arrowheads in **a** indicate Pax7⁺ satellite cells. Arrowheads in **c** indicate CD31⁺ capillary endothelium surrounded by basement membrane. Scale bars, 10 μm **(a, b, d)**, 5 μm **(c)** and 20 μm **(e)**.

to differentiate into adipocytes[20], we studied the relationship between PDGFRα⁺ cells and pericytes. The definition of pericytes is based on their anatomic location; pericytes are bound by the same basement membrane as capillary endothelial cells. PDGFRα⁺ cells were found to reside outside the capillary basement membrane (Fig. 3c) and they did not express NG2, a pericyte marker (Fig. 3d), indicating that they are distinct from pericytes. PDGFRα⁺ cells were more frequently observed in the perimysium than in the endomysium. They tended to localize circumferentially around vessels, but could be distinguished from vascular smooth muscle cells by the absence of α-smooth muscle actin (αSMA) staining (Fig. 3e).

Behaviour of PDGFRα⁺ cells during fatty degeneration of skeletal muscle

We next sought to examine the contribution of PDGFRα⁺ cells to *in vivo* fat formation in skeletal muscle. In mice, however, the occurrence of adipocytes in skeletal muscle is rare, even in pathologic mouse models such as *mdx*, DMD or obese mice. We therefore used a muscle injury model induced by injection with glycerol, which has been reported to induce destabilization of the cytoplasmic membrane followed by cell death, and eventually results in fatty degeneration of the injected muscle[21]. This model has been used to evaluate the efficacy of gene therapy for muscular disorders[21]. When glycerol was injected into the tibialis anterior muscle of C57BL/6 mice, we confirmed that muscle fibre disruption was followed by the development of adipocytes at ~7 days after injection, and a subsequent increase in fatty and fibrous connective tissue particularly in the peripheral regions of injected muscle on day 14 (Fig. 4a). Adipose cells then gradually decreased in number, but could be observed at least 1 month after injury (data not shown). We examined the behaviour of endogenous PDGFRα⁺ cells during this degeneration process. Many proliferating PDGFRα⁺ cells were observed in the interstitial space 4 days after injury (Fig. 4b). However, we could not detect expression of PDGFRα in adipocytes that had arisen in muscle on day 7 (Fig. 4c).

Only the PDGFRα⁺ population can differentiate into adipocytes in glycerol-injected fatty degenerating muscle

Given that purified PDGFRα⁺ cells lost PDGFRα expression after adipogenic differentiation *in vitro*, it was assumed that interstitial PDGFRα⁺ cells proliferate and then differentiate into adipocytes while downregulating PDGFRα. To confirm this, we transplanted cells isolated from muscles of GFP transgenic (Tg) mice into tibialis anterior muscles of wild type mice that had been injected with glycerol. Three freshly isolated cell populations, a mixed population of CD31⁺ and CD45⁺ cells, CD31⁻CD45⁻PDGFRα⁻ cells and CD31⁻CD45⁻PDGFRα⁺ cells, were transplanted immediately after cell sorting (Fig. 5a). Pax7 expression revealed by cytospin was detected only in CD31⁻CD45⁻PDGFRα⁻ cells, indicating that satellite cells were sorted in this population (data not shown). At day 14, few GFP⁺ cells were observed in muscles that had been injected with the mixed population of CD31⁺ and CD45⁺ cells (Fig. 5b). In CD31⁻CD45⁻PDGFRα⁻ cell- or CD31⁻CD45⁻PDGFRα⁺ cell-transplanted muscles, numerous GFP⁺ cells were detected (Fig. 5b). The expression of myosin heavy chain (MyHC) indicated that CD31⁻CD45⁻PDGFRα⁻ cells differentiated into myofibres (Fig. 5c). Differentiation of transplanted CD31⁻CD45⁻PDGFRα⁺ cells into mature adipocytes was confirmed by the expression of both C/EBPα and PPARγ, and the presence of a single large lipid vacuole (Fig. 5d). Quantitative analysis revealed that the myogenic potential was found exclusively in the CD31⁻CD45⁻PDGFRα⁻ population, whereas adipocytes arose only from CD31⁻CD45⁻PDGFRα⁺ cells (Fig. 5e). These results suggest that only CD31⁻CD45⁻PDGFRα⁺ cells can differentiate into adipocytes *in vivo*. To further confirm this notion, we investigated whether bone marrow-derived cells contribute to *in vivo* adipocyte formation in skeletal muscle using bone marrow chimaeric mice. Bone marrow-derived cells did not give rise to either PDGFRα⁺ cells or to adipocytes during adipogenesis induced by glycerol injection (Supplementary Information, Fig. S9). Collectively, our data suggest that muscle-resident interstitial PDGFRα⁺ cells are the sole source of adipocytes that arise in skeletal muscle in the context of glycerol-induced fatty degeneration.

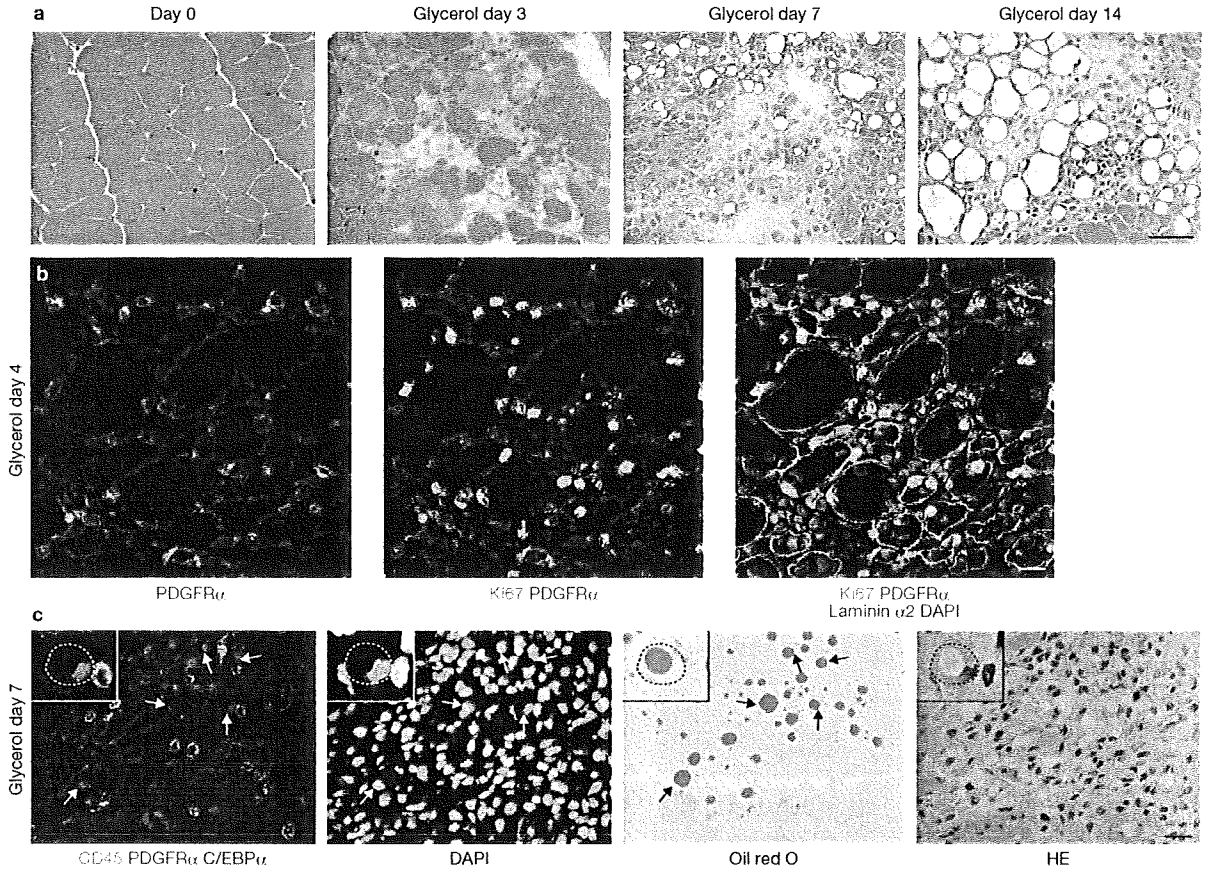

Figure 4 Behaviour of PDGFRα⁺ cells in fatty degenerating muscle. (**a**) Histological changes in skeletal muscle was analysed by hematoxylin and eosin (HE) staining during glycerol-induced fatty degeneration. *Tibialis anterior* muscles were injected with glycerol and, at the time points indicated, frozen muscle sections were subjected to HE staining. (**b**) Four days after glycerol injection, muscle sections were stained with anti-PDGFRα, anti-Ki67 and anti-laminin α2 antibodies. (**c**) On day 7 after glycerol injection, muscle sections were subjected to immunofluorescence staining for CD45, PDGFRα and C/EBPα, and subsequently to oil red O staining followed by HE staining. C/EBPα⁺ oil red O⁺ unilocular adipocytes were negative for CD45 and PDGFRα (arrows and insets). Scale bars, 50 μm (**a**) and 20 μm (**b**, **c**).

The fate of PDGFRα⁺ cells is largely dependent on the muscle environment

To understand how *in vivo* adipogenesis of PDGFRα⁺ cells is regulated, we used a muscle regeneration model induced by cardiotoxin (CTX) injection. In contrast to glycerol injection, CTX injection rarely induces adipocyte formation in the skeletal muscle of C57BL/6 mice. Thus, it is expected that the behaviour of PDGFRα⁺ cells in CTX-injected muscle is regulated in a manner distinct to those in muscle with a glycerol-induced injury. Intriguingly, PDGFRα⁺ cells significantly increased in number in CTX-induced regenerating muscle as well as in glycerol-injected degenerating muscle (Fig. 6a). However, the number of PDGFRα⁺ cells decreased without differentiating into adipocytes as muscle regeneration proceeded (Fig. 6a). We isolated proliferating PDGFRα⁺ cells from both CTX-injected and glycerol-injected muscles and compared their adipogenic potentials. Both were largely negative for C/EBPα immediately after isolation (Fig. 6b). Surprisingly, they showed comparable levels of adipogenic potential under adipogenic culture conditions (Fig. 6c, d). Thus, non-cell-autonomous mechanisms are likely to determine the differences between cell fate resulting from CTX injection and glycerol injection. To test this directly, we performed reciprocal transplantations between regenerating and degenerating muscles (Fig. 7a). If the adipogenic fate of PDGFRα⁺ cells is already determined at day 4 of glycerol injection, PDGFRα⁺ cells isolated from glycerol-injected muscle should form adipocytes, even in CTX-injected regenerating muscle, in a cell-autonomous manner. If the muscle environment determines PDGFRα⁺ cell adipogenic fate, PDGFRα⁺ cells isolated from CTX-injected muscle should adapt their fate to an adipocyte lineage in glycerol-injected muscle. The results demonstrate that the latter is the case. PDGFRα⁺ cells isolated from glycerol-injected muscle did not differentiate into adipocytes in CTX-injected muscle, where only a few transplanted cells were observed that were similar to endogenous PDGFRα⁺ cells (Fig. 7b, e). In contrast, PDGFRα⁺ cells isolated from CTX-injected muscle accumulated in degenerated areas and differentiated into C/EBPα⁺PPARγ⁺, lipid-laden adipocytes in glycerol-injected muscle (Fig. 7c–e). These results clearly show that the fate of PDGFRα⁺ cells is largely regulated by the surrounding muscle environment.

Muscle fibres have a strong inhibitory effect on the adipogenesis of PDGFRα⁺ cells

Our results indicate that the muscle environment after the fourth day of CTX injection has an inhibitory effect on adipogenesis of PDGFRα⁺ cells,

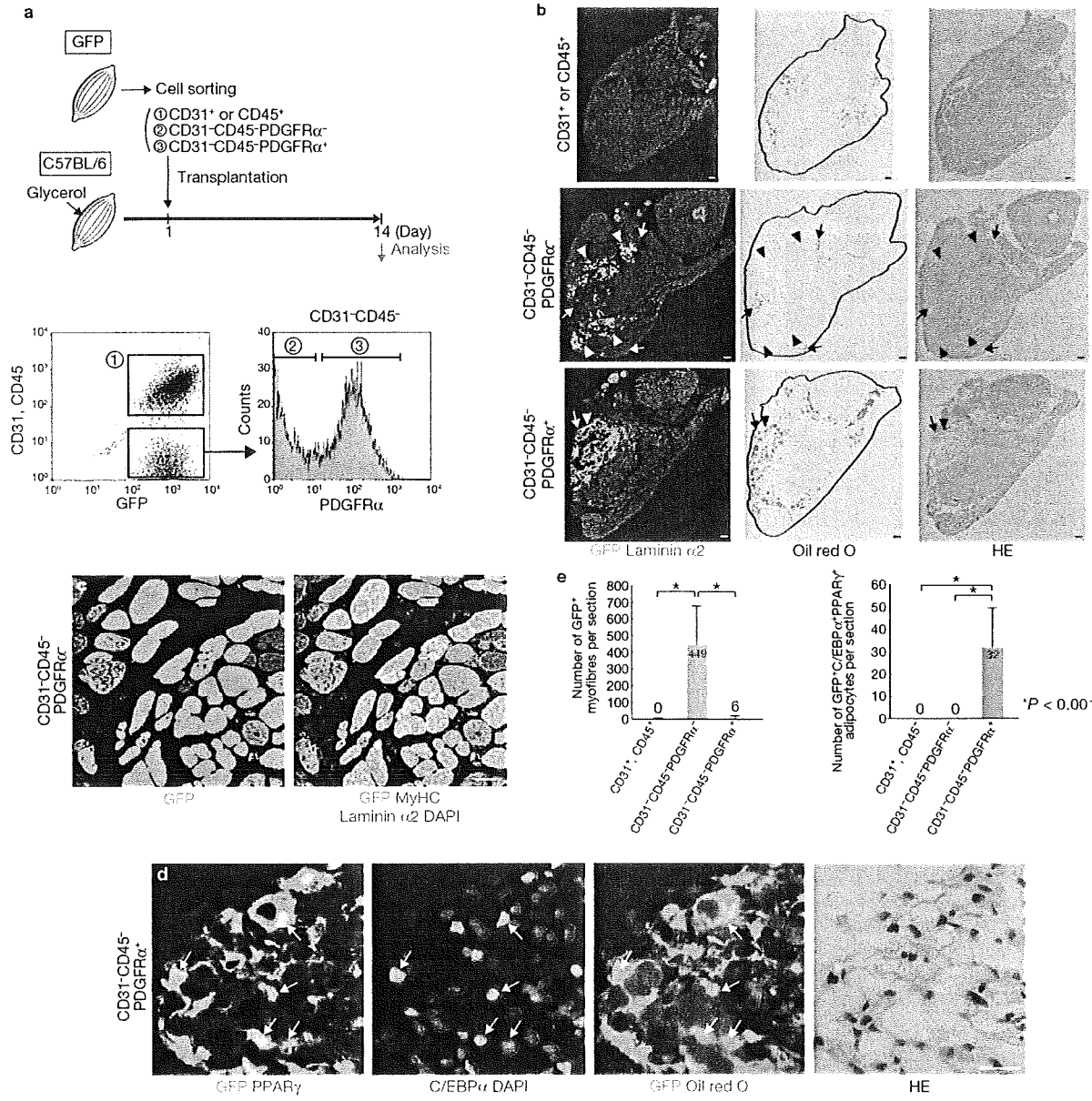

Figure 5 Only PDGFRα+ cells differentiate into adipocytes after transplantation into glycerol-injured muscle. (**a**) Transplantation procedures. (**b**) On day 14 after glycerol injection, transplanted muscle sections were subjected to immunofluorescence staining for GFP and laminin α2, and subsequently to oil red O staining followed by hematoxylin and eosin (HE) staining. Arrowheads indicate GFP+ area. Arrows indicate oil red O+ fatty degenerated area. (**c**) CD31-CD45-PDGFRα- cell-transplanted muscles were analysed for expression of GFP, MyHC and laminin α2. (**d**) Sections of CD31-CD45-PDGFRα+ cell-transplanted muscles were subjected to immunofluorescence staining for GFP, C/EBPα and PPARγ, and subsequently to oil red O staining followed by HE staining. Arrows indicate GFP+C/EBPα+PPARγ+ oil red O+ unilocular adipocytes. (**e**) Quantitative analysis of transplantation experiments. Error bars indicate the mean ± s.d., $n = 6$ in each group. Scale bars, 100 μm (**b**) and 20 μm (**c**, **d**).

whereas the muscle environment after the fourth day of glycerol injection facilitates adipogenesis. Active differentiation of myogenic cells and new myofibre formation occurs after day 4 of CTX injection[22]. Therefore, we examined myogenic differentiation in both CTX and glycerol models. Administration of 5-ethynyl-2′-deoxyuridine (EdU) in combination with embryonic MyHC (eMyHC) staining was performed to analyse *de novo* myofibre formation. Five days after injury, much higher numbers of eMyHC+EdU+ new myofibres were observed in CTX-injected muscles compared with glycerol-injected muscles (Fig. 8a, b, e). Myogenin staining further revealed that muscle regeneration was severely compromised in glycerol-injected muscles (Fig. 8c–e). At this time point, PDGFRα+ cells showing an elongated spindle shape were distributed in the narrow space between regenerating myofibres in CTX-injected muscles, whereas many PDGFRα+ cells were observed in the extended interstitial space between degenerating myofibres and showed an enlarged rounded morphology in glycerol-injected muscles (Fig. 8c, d). This impairment